



Article

An Innovative Approach to a Potential Neuroprotective *Sideritis scardica*-Clinoptilolite Phyto-Nanocarrier: In Vitro Investigation and Evaluation

Adina-Elena Segneanu ^{1,*} , Gabriela Vlase ^{1,2}, Titus Vlase ^{1,2} , Andrei Bită ³ , Cornelia Bejenaru ⁴, Gabriela Buema ⁵, Ludovic Everard Bejenaru ³, Andrei Dumitru ⁶ and Eugen Radu Boia ⁷

- ¹ Institute for Advanced Environmental Research-West University of Timisoara (ICAM-WUT), Oituz nr.4, 300223 Timisoara, Romania; gabriela.vlase@e-uvt.ro (G.V.); titus.vlase@e-uvt.ro (T.V.)
 - ² Research Centre “Thermal Anal Environm Problems”, Institute for Advanced Environmental Research-West University of Timisoara (WUT), Pestalozzi St 16, 300115 Timisoara, Romania
 - ³ Department of Pharmacognosy & Phytotherapy, Faculty of Pharmacy, University of Medicine and Pharmacy Craiova, St. Petru Rareș 2, 200349 Craiova, Romania; andrei.bită@umfcv.ro (A.B.)
 - ⁴ Department of Pharmaceutical Botany, Faculty of Pharmacy, University of Medicine and Pharmacy Craiova, St. Petru Rareș 2, 200349 Craiova, Romania; cornelia.bejenaru@umfcv.ro
 - ⁵ National Institute of Research and Development for Technical Physics, 47 Mangeron Boulevard, 700050 Iasi, Romania; gbuema@phys-iasi.ro
 - ⁶ Faculty of Sciences, Physical Education and Informatics—Department of Medical Assistance and Physiotherapy, National University for Science and Technology Politehnica Bucharest, University Center of Pitesti, Targu din Vale 1, 110040 Pitesti, Romania; andrei.dumitru@upit.ro
 - ⁷ Department of Ear, Nose, and Throat, Faculty of Medicine, “Victor Babeș” University of Medicine and Pharmacy Timisoara, 2 Eftimie Murgu, 300041 Timisoara, Romania; eugen.boia@umft.ro
- * Correspondence: adina.segneanu@e-uvt.ro



Citation: Segneanu, A.-E.; Vlase, G.; Vlase, T.; Bită, A.; Bejenaru, C.; Buema, G.; Bejenaru, L.E.; Dumitru, A.; Boia, E.R. An Innovative Approach to a Potential Neuroprotective *Sideritis scardica*-Clinoptilolite Phyto-Nanocarrier: In Vitro Investigation and Evaluation. *Int. J. Mol. Sci.* **2024**, *25*, 1712. <https://doi.org/10.3390/ijms25031712>

Academic Editor: David Della-Morte

Received: 23 December 2023

Revised: 25 January 2024

Accepted: 27 January 2024

Published: 30 January 2024



Copyright: © 2024 by the authors. Licensee MDPI, Basel, Switzerland. This article is an open access article distributed under the terms and conditions of the Creative Commons Attribution (CC BY) license (<https://creativecommons.org/licenses/by/4.0/>).

Abstract: The cutting-edge field of nanomedicine combines the power of medicinal plants with nanotechnology to create advanced scaffolds that boast improved bioavailability, biodistribution, and controlled release. In an innovative approach to performant herb nanoproducts, *Sideritis scardica* Griseb and clinoptilolite were used to benefit from the combined action of both components and enhance the phytochemical’s bioavailability, controlled intake, and targeted release. A range of analytical methods, such as SEM-EDX, FT-IR, DLS, and XDR, was employed to examine the morpho-structural features of the nanoproducts. Additionally, thermal stability, antioxidant screening, and in vitro release were investigated. Chemical screening of *Sideritis scardica* Griseb revealed that it contains a total of ninety-one phytoconstituents from ten chemical categories, including terpenoids, flavonoids, amino acids, phenylethanoid glycosides, phenolic acids, fatty acids, iridoids, sterols, nucleosides, and miscellaneous. The study findings suggest the potential applications as a promising aspirant in neurodegenerative strategy.

Keywords: ironwort; zeolite; phytochemicals; drug delivery systems; antioxidant potential; dissolution profile

1. Introduction

Sideritis scardica Griseb (*Lamiaceae* family) has been known for its medicinal properties since ancient times. Renowned scholars and physicians such as Hippocrates, Discorides, Theophrastus, and Galen have recommended this plant for wound regeneration and healing caused by iron weapons. In Southeast Europe and Turkey, the plant is used for flavoring or preparing tea, hence its common name, ironwort or “Mountain tea” [1,2]. In addition, there are other local names for this plant. For instance, in Bulgaria, it is known as “Pirin tea”, “Mursalski tea”; or “Alibotushki tea”. In Greece, it is referred to as “Greek Mountain tea” or “Olympus tea”, while in North Macedonia, it is called “Sharplaninsi čaj” [1–3]. *Sideritis scardica* is highly valued in traditional medicine in these regions and is considered one

of the most famous herbs, known for its astonishing therapeutic properties such as antioxidant, anti-inflammatory, anti-ulcerogenic, digestive, and antimicrobial effects. Recent research reported the notable biological activity (antiseptic, diaphoretic, anti-rheumatic, gastroprotective, antidiabetic, antiproliferative, anti-HIV, and neuroprotective) because of the collective action of its highly complex phytoconstituents composition [1,3–5].

Current studies have focused on the development of nanomaterials development derived from natural compounds to overcome the *in vivo* limitations of some secondary metabolites. These limitations may include chemical or thermal instability, poor bioavailability, limited membrane phytoconstituents transport, and others. Through the creation of nanomaterials, prolonged action, vectorization, specificity, and superior therapeutic action can be achieved [6–10].

Clinoptilolite-zeolite is a widely available, low-cost, crystalline hydrated aluminosilicate with a unique structure, regular microporous, high thermal and chemical stability, and high ion exchange selectivity. Due to their extraordinary morpho-structural properties, clinoptilolite has proven to be a highly versatile material with numerous potential applications across various fields, including agriculture, industry, catalysts, environmental protection, and biomedicine. Studies have also shown that this mineral can have several beneficial effects on human health, such as anti-inflammatory, antioxidant, antibacterial, antitumoral immunomodulating agent, and protecting against neurodegenerative diseases [11–17]. Recent research has demonstrated their efficacy in various medical applications (biosensors, diagnosis, drug delivery systems, bone tissue engineering, detoxification, dental treatments, and more) [11–17]. Although clinoptilolite's possible side effects were controversial issues concerning therapeutic uses, the latest research reported that micronized eliminates these shortcomings and increases the efficiency of biomedical applications [12,13]. Numerous literature results report that clinoptilolite exhibits remarkable potential as a carrier platform, owing to its ability to significantly enhance both the shelf life and biocompatibility of phytoconstituents *in vivo*, thereby facilitating controlled and prolonged release [11,13,15,18–20]. Specifically, the unique physicochemical properties of clinoptilolite have been shown to effectively stabilize and protect phytoconstituents from degradation and toxicity while also improving their bioavailability and therapeutic efficacy [11,13,15,18–20]. These findings suggest that clinoptilolite represents a promising platform for the development of advanced drug delivery systems that can overcome many of the limitations associated with conventional drug delivery methods [11,19,20].

Nevertheless, as the importance of safe and effective self-medication increases worldwide, the need to explore alternatives to traditional drugs is becoming more pressing. Medicinal plant preparations offer a compelling opportunity, providing beneficial health effects, treating ailments, and boosting immunity through their potent antioxidant, antimicrobial, antiviral, anti-inflammatory, and antitumor properties. However, research has indicated that self-administration of herbal products can result in exceeding optimal doses, leading to severe complications [21–26]. Therefore, the highly effective herb product development that addresses these concerns by providing controlled intake and release of biomolecules, increasing bioavailability, and minimizing toxicity is paramount. Accordingly, herbal products can offer a safe and effective solution to the problem of antibiotic resistance and harmful side effects associated with traditional drugs.

To this end, this study uses a novel, simple approach for developing a new carrier system that combines ironwort and clinoptilolite to harness their collective action. The physicochemical properties, antioxidant potential, and *in vitro* dissolution test of this new nanocarrier were investigated thoroughly.

2. Results and Discussion

Various studies focused on the chemical screening and biological activity of *Sideritis scardica*, one of the most famous medicinal plants in the Balkan region. Nevertheless, variation in the chemical composition of a plant depending on numerous biotic, abiotic, and experimental parameters greatly complicates the establishment of an interdependence

between the biological activity of a medicinal plant and the profile of secondary metabolites [27,28].

Numerous studies have reported that several phytoconstituents with outstanding biological activity exhibit in vivo reduced adsorption and reduced permeability, corresponding to their size, solubility, and stability (thermal and chemical). The limited target specificity, transmembrane permeability, and retention of these compounds also represent significant obstacles to current therapeutic strategies for severe diseases [28–31].

Nonetheless, identifying and addressing these challenges will lead to the development of effective treatments for severe diseases [31]. Therefore, innovative approaches are imposed to overcome these challenges.

Conversely, certain phytoconstituents isolation and then their total chemical synthesis or semi-synthesis are essential and challenging steps related to the complex chemical structure (stereochemical centers, and others) [27,28,32,33]. Nevertheless, the latest literature results have shown that the combined therapeutic effects of all secondary metabolites in a whole plant are superior to the biological activity of a single biomolecule [27,28,32,33]. Accordingly, the design of phytocarrier systems that combine the biological action of all secondary metabolites from a medicinal plant and that of the carrier can overcome the current therapeutic strategy limitations and allow controlled release and target specificity.

Complete screening of low-weight phytoconstituents from ironwort sample was performed using gas-chromatography coupled with mass spectroscopy (GC-MS) and electro-spray ionization–quadrupole time-of-flight mass spectrometry (ESI-QTOF-MS) techniques.

Gas chromatography coupled with mass spectrometry (GC-MS) is one of the most common, fast, and easy techniques for the specific identification of volatile molecules from a complex mixture [34].

However, non-volatile and or thermolabile metabolites require additional methods of protection by chemical derivatization before GC-MS analysis [35].

2.1. Screening of Amino Acid from *Sideritis Scardica* Sample

The amino acid profile from the ironwort sample was investigated using GC-MS techniques (Figure 1). The compounds were identified based on the retention indices, mass spectra with those of NIST/EPA/NIH, the Mass Spectral Library 2.0 database, and the literature [36–38].

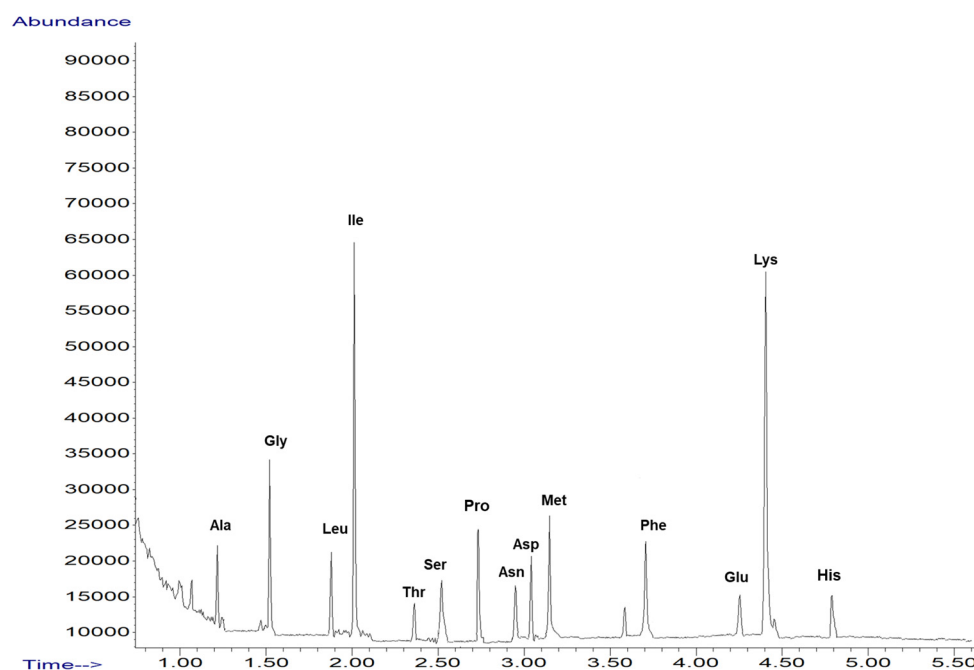


Figure 1. TIC chromatograms of GC-MS for *Sidertis scardica*.

Table 1 presents the tentative amino acid identification via GC-MS corresponding to the *Sideritis scardica* sample.

Table 1. GC-MS amino acids identification from *Sideritis scardica* sample.

Proposed Structure	Abbreviation	SIM (Selected Ion Monitoring)
alanine	Ala	130, 70
glycine	Gly	116, 74
leucine	Leu	172, 86
isoleucine	Ile	172, 130
threonine	Thr	160, 101
serine	Ser	146, 203
proline	Pro	156, 243
asparagine	Asn	155, 69
aspartic acid	Asp	216, 130
methionine	Met	203, 277
phenylalanine	Phe	206, 190
glutamic acid	Glu	230, 170
lysine	Lys	170, 128
histidine	His	282, 168

2.2. Mass Spectrometry Analysis of *Sideritis Scardica* Sample

The MS results depicted a highly heterogenous composition of compounds, of which some were detected, as pertaining to several chemical categories (amino acids, terpenoids, iridoids, phenylethanoid glycosides, sterols, fatty acids, flavonoids, phenolic acids, and others) that confirmed the data reported in the literature [37,39–50].

The mass spectrum and the biomolecules identified via ESI-QTOF-MS analysis are shown in Figure 2 and Table 2, respectively.

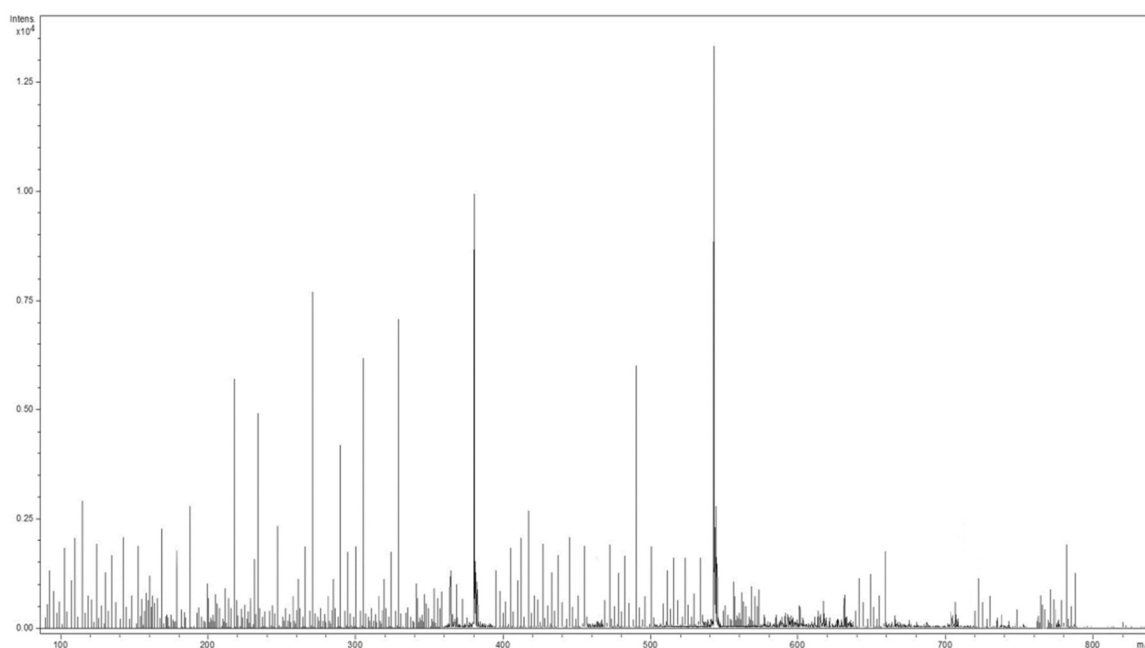


Figure 2. The mass spectra of *Sideritis scardica*.

Table 2. Biomolecules identified in *Sideritis scardica* sample through MS analysis.

No	Detected <i>m/z</i>	Theoretic <i>m/z</i>	Formula	Tentative of Identification	Category	Ref.
1	76.08	75.07	C ₂ H ₅ NO ₂	glycine	amino acids	[37,38,51]
2	90.11	89.09	C ₃ H ₇ NO ₂	alanine		[37]
3	106.07	105.09	C ₃ H ₇ NO ₃	serine		[37]
4	116.11	115.13	C ₅ H ₉ NO ₂	proline		[37]
5	120.13	119.12	C ₄ H ₉ NO ₃	threonine		[37]
6	132.15	131.17	C ₆ H ₁₃ NO ₂	isoleucine		[37]
7	133.13	132.12	C ₄ H ₈ N ₂ O ₃	asparagine		[37]
8	134.11	133.10	C ₄ H ₇ NO ₄	aspartic acid		[37]
9	147.18	146.19	C ₆ H ₁₄ N ₂ O ₂	lysine		[37,38,51]
10	148.14	147.13	C ₅ H ₉ NO ₄	glutamic acid		[37]
11	149.23	149.21	C ₅ H ₁₁ NO ₂ S	methionine		[37,38,51]
12	156.17	155.15	C ₆ H ₉ N ₃ O ₂	histidine		[37,38,51]
13	166.17	165.19	C ₉ H ₁₁ NO ₂	phenylalanine		[37]
14	271.25	270.24	C ₁₅ H ₁₀ O ₅	apigenin		flavonoids
15	285.27	284.26	C ₁₆ H ₁₂ O ₅	genkwanin	[41]	
16	287.23	286.24	C ₁₅ H ₁₀ O ₆	luteolin	[45,46,48]	
17	301.27	300.26	C ₁₆ H ₁₂ O ₆	chrysoeriol	[5,45,48]	
18	303.25	302.23	C ₁₅ H ₁₀ O ₇	hypolaetin	[48]	
19	315.28	314.29	C ₁₇ H ₁₄ O ₆	cirsimaritin	[41,49]	
20	317.25	316.26	C ₁₆ H ₁₂ O ₇	nepetin	[49]	
21	329.28	328.30	C ₁₈ H ₁₆ O ₆	salvigenin	[49]	
22	343.35	342.34	C ₁₆ H ₂₂ O ₈	coniferin	[41]	
23	345.21	344.22	C ₁₈ H ₁₆ O ₇	eupatorin	[41]	
24	651.61	650.60	C ₃₀ H ₃₄ O ₁₆	tremasperin	[41]	
25	165.17	164.16	C ₉ H ₈ O ₃	<i>p</i> -coumaric acid	phenolic acids	[45]
26	169.14	168.15	C ₈ H ₈ O ₄	vanillic acid		[45]
27	171.13	170.12	C ₇ H ₆ O ₅	gallic acid		[45]
28	181.15	180.16	C ₉ H ₈ O ₄	caffeic acid		[45]
29	193.15	192.17	C ₇ H ₁₂ O ₆	quinic acid		[48]
30	195.17	194.18	C ₁₀ H ₁₀ O ₄	ferulic acid		[45]
31	199.15	198.17	C ₉ H ₁₀ O ₅	syringic acid		[45]
32	355.33	354.31	C ₁₆ H ₁₈ O ₉	chlorogenic acid		[5,45]
33	135.21	134.22	C ₁₀ H ₁₄	<i>o</i> -cymene	terpenoids	[42]
34	137.24	136.23	C ₁₀ H ₁₆	α -thujene		[43,44]
35	149.19	148.20	C ₁₀ H ₁₂ O	anethone		[43]
36	151.21	150.22	C ₁₀ H ₁₄ O	tymol		[43]
37	153.25	152.23	C ₁₀ H ₁₆ O	camphor		[43]
38	154.25	154.25	C ₁₀ H ₁₈ O	borneol		[43]
39	157.25	156.26	C ₁₀ H ₂₀ O	menthol		[43]

Table 2. Cont.

No	Detected <i>m/z</i>	Theoretic <i>m/z</i>	Formula	Tentative of Identification	Category	Ref.
40	191.27	190.28	C ₁₃ H ₁₈ O	damascenone	terpenoids	[47]
41	193.31	192.30	C ₁₃ H ₂₀ O	beta-damascone		[43]
42	199.31	198.30	C ₁₅ H ₁₈	cadalene		[43]
43	202.34	202.33	C ₁₅ H ₂₂	α-curcumene		[46]
44	205.35	204.35	C ₁₅ H ₂₄	humulene		[43]
45	219.31	218.33	C ₁₅ H ₂₂ O	germacrone		[48]
46	221.34	220.35	C ₁₅ H ₂₄ O	spatulenol		[40,43]
47	223.36	222.37	C ₁₅ H ₂₆ O	valeranone		[43]
48	297.49	296.50	C ₂₀ H ₄₀ O	phytol		[43]
49	305.49	304.50	C ₂₀ H ₃₂ O ₂	sideridiol		[45]
50	321.49	320.50	C ₂₀ H ₃₂ O ₃	sideroxol		[45,48]
51	323.51	322.50	C ₂₀ H ₃₄ O ₃	andalusol		[49]
52	333.41	332.40	C ₂₀ H ₂₈ O ₄	carnosic acid		[41]
53	347.49	346.50	C ₂₂ H ₃₄ O ₃	siderol		[45,48]
54	363.51	362.50	C ₂₂ H ₃₄ O ₄	eubol	[45,48]	
55	463.41	462.40	C ₂₀ H ₃₀ O ₁₂	forsythoside	[48]	
56	625.59	624.60	C ₂₉ H ₃₆ O ₁₅	verbascoside	[5]	
57	639.58	638.60	C ₃₀ H ₃₈ O ₁₅	leucosceptoside A	[48,50]	
58	653.58	652.60	C ₃₁ H ₄₀ O ₁₅	martynoside	phenylethanoid glycosides	[48,50]
59	669.62	668.60	C ₃₁ H ₄₀ O ₁₆	verbascoside		[48]
60	757.71	756.70	C ₃₄ H ₄₄ O ₁₉	lavandulifolioside		[48,50]
61	771.68	770.70	C ₃₅ H ₄₆ O ₁₉	alyssonoside		[48,50]
62	787.70	786.70	C ₃₅ H ₄₆ O ₂₀	echinacoside	[48,50]	
63	375.33	374.34	C ₁₆ H ₂₂ O ₁₀	geniposidic acid	iridoids	[41]
64	449.39	448.40	C ₁₉ H ₂₈ O ₁₂	barlerin		[41]
65	525.51	524.50	C ₂₁ H ₃₂ O ₁₅	melittoside		[42]
66	173.27	172.26	C ₁₀ H ₂₀ O ₂	capric acid	fatty acids	[43]
67	201.33	200.32	C ₁₂ H ₂₄ O ₂	lauric acid		[43]
68	257.41	256.42	C ₁₆ H ₃₂ O ₂	palmitic acid		[43]
69	281.39	280.40	C ₁₈ H ₃₂ O ₂	linoleic acid		[43]
70	283.51	282.50	C ₁₈ H ₃₄ O ₂	oleic acid		[43,46]
71	401.69	400.70	C ₂₈ H ₄₈ O	campesterol	sterols	[48]
72	413.69	412.70	C ₂₉ H ₄₈ O	stigmasterol		[48]
73	415.71	414.70	C ₂₉ H ₅₀ O	β sitosterol		[48]
74	245.21	244.20	C ₉ H ₁₂ N ₂ O ₆	uridine	nucleosides	[41]
75	284.25	283.24	C ₁₀ H ₁₃ N ₅ O ₅	guanine	nucleosides	[41]
76	103.15	102.17	C ₆ H ₁₄ O	hexanol	alcohols	[40]
77	129.19	128.21	C ₈ H ₁₆ O	oct-1-en-3-ol		[40]
78	271.49	270.50	C ₁₈ H ₃₈ O	2-octadecanol		[43]

Table 2. Cont.

No	Detected m/z	Theoretic m/z	Formula	Tentative of Identification	Category	Ref.
79	207.27	206.28	C ₁₃ H ₁₈ O ₂	hexylbenzoate	esters	[39]
80	213.25	212.24	C ₁₄ H ₁₂ O ₂	benzylbenzoate		[39]
81	295.51	294.50	C ₁₉ H ₃₄ O ₂	methyl lineoleate		[43]
82	313.51	312.50	C ₂₀ H ₄₀ O ₂	stearyl acetate		[39]
83	143.27	142.28	C ₁₀ H ₂₂	decane	hydrocarbons	[43]
84	325.59	324.60	C ₂₃ H ₄₈	tricosane		[43]
85	353.71	352.70	C ₂₅ H ₅₂	pentacosane		[43]
86	121.17	120.15	C ₈ H ₈ O	acetophenone	ketones	[40]
87	165.25	164.24	C ₁₁ H ₁₆ O	cis-jasmone		[46]
88	123.11	122.12	C ₇ H ₆ O ₂	benzoic acid	organic acids	[40]
89	135.07	134.09	C ₄ H ₆ O ₅	malic acid		[41]
90	151.07	150.09	C ₄ H ₆ O ₆	tartaric acid		[41]
91	201.21	200.23	C ₁₀ H ₁₆ O ₄	camphoric acid		[42]

2.3. Screening and Classification of the Differential Metabolites

A total of 91 secondary phytochemicals identified through mass spectroscopy were assigned to different chemical classes: terpenoids (24.18%), flavonoids (12.08%), amino acids (14.28%), phenylethanoid glycosides (8.8%), phenolic acids (8.8%), fatty acids (5.5%), iridoids (3.3%), sterols (3.3%), nucleosides (2.2%) and miscellaneous.

Figure 3 presents the classification chart of the phytoconstituents from the *Sideritis scardica* sample based on the data analysis reported in Table 2.

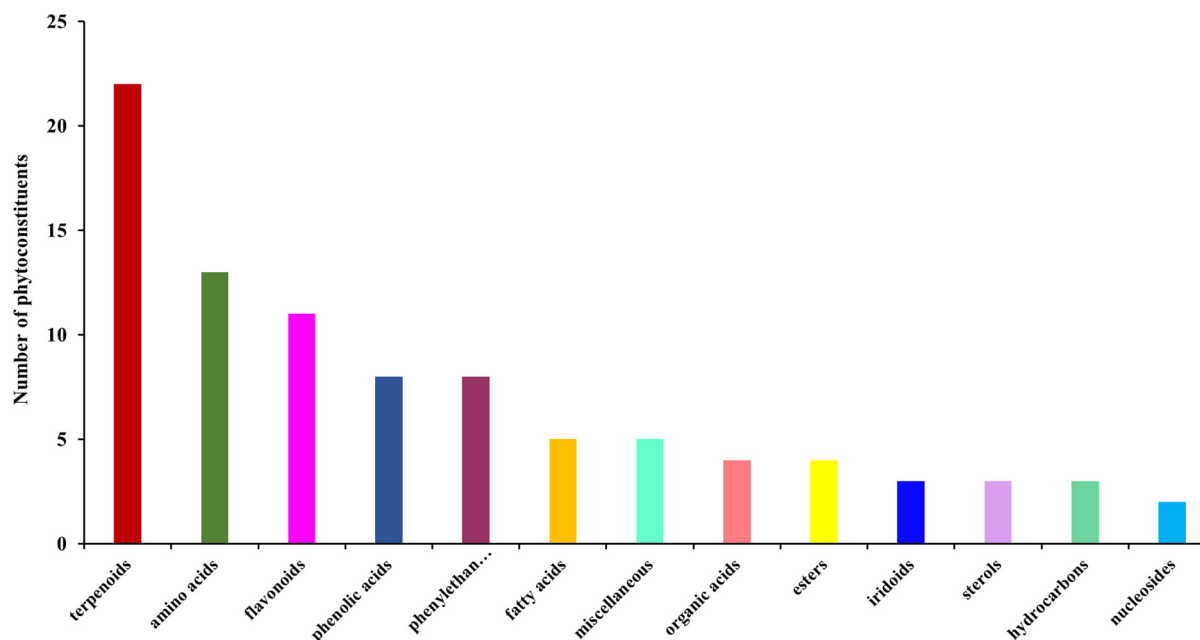


Figure 3. Phytochemical classification bar chart for *Sideritis scardica*.

According to Figure 3, terpenoids represent the biggest class of secondary metabolites, comprising about 24.18%. Various research reported their remarkable biological properties: anti-inflammatory, antitumor, analgesic, antimicrobial, antiviral, neuroprotective, antispasmodic, antihyperglycemic, antiplasmodial, cardioprotective, and immunomodulatory [52].

Flavonoids are a category of metabolites with noteworthy therapeutic activity: antioxidant, anti-inflammatory, cardioprotective, neuroprotective, antimicrobial, antiviral, and antitumoral [53,54].

Amino acids play a crucial role in maintaining the overall human health. In the ironwort sample, a total of eleven compounds were identified, with essential and non-essential amino acids present in almost equal proportions. The therapeutic properties of amino acids have been extensively studied in biochemistry. Recent research has shown that a significant portion of the amino acids identified in the ironwort sample (over 46% of all amino acids identified) such as isoleucine, glycine, alanine, histidine, phenylalanine, and glutamic acid, exhibit antiproliferative, cytotoxic, and immunomodulating activities [55–58]. Additionally, amino acids like methionine, proline serine, lysine, threonine, and asparagine have been found to possess anti-inflammatory properties [59–63].

In addition, lysine exerts neuroprotection activity and serine cytoprotective and antiatherogenic effects [64,65].

Phenylethanoid glycosides (PhGs) are metabolites with notable biological activities (antioxidant, antibacterial and neuroprotective) [66].

Phenolic acids represent 9% of the phytoconstituents from the ironwort sample. Numerous research have demonstrated their pharmacological activity (antioxidant, antimicrobial, cardioprotective, anti-inflammatory, neuroprotective, antitumor, and antidiabetic) [67].

Iridoids act as neuroprotective, hepatoprotective, anti-inflammatory, antitumor, hypoglycaemic, and hypolipidemic agents [68].

Nucleosides uridine and guanosidine act as neuroprotective, neuromodulator, and neurodegenerative agents [69,70].

Fatty acids represent 5.5% of the metabolites from the ironwort sample. Recent studies reported their cardioprotective, anti-inflammatory, antioxidant, and neuroprotective effects [71,72].

Phytosterols in the proportion of about 3.4% from biomolecule categories identified in ironwort samples have demonstrated antioxidant, anti-inflammatory, neuroprotective, immunomodulatory, and antitumoral [73].

2.4. Phyto-Nanocarrier System

Numerous studies have reported that several phytoconstituents with outstanding biological activity exhibit in vivo reduced adsorption and reduced permeability because of their size, solubility, and stability (thermal and chemical) [74].

The limited target specificity, transmembrane permeability, and retention of these compounds also represent significant obstacles to current therapeutic strategies for severe diseases. Nonetheless, identifying and addressing these challenges will lead to the development of effective treatments for severe diseases. Therefore, innovative approaches are imposed to overcome these challenges [31,75,76]. Consequently, the development of an advanced phyto-nanocarrier system by loading secondary metabolites from *Sideritis scardica* into clinoptilolite particles combines the biological activity of the phytoconstituents and the carrier enhancing the therapeutical performance (pharmacological effects, selectivity, controlled released, and bioavailability).

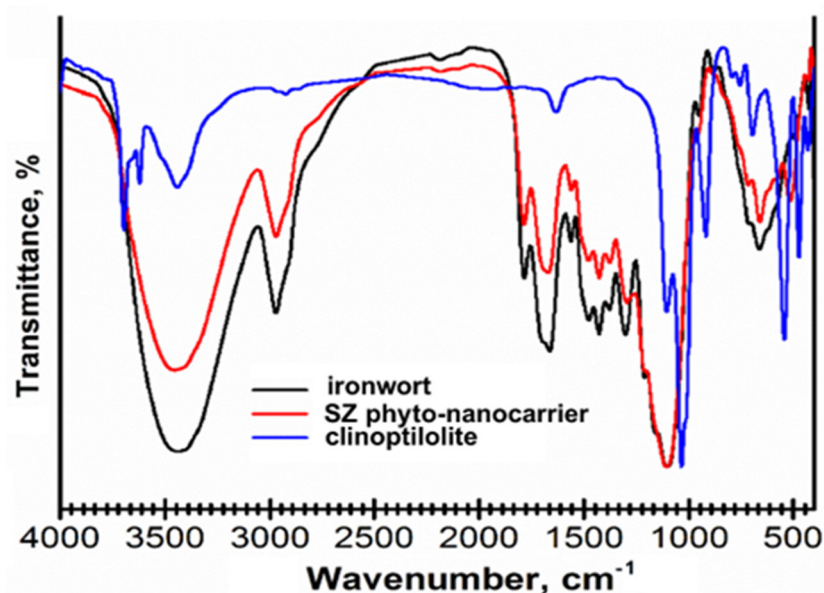
2.4.1. FT-IR Spectroscopy

Fourier transform infrared (FT-IR) spectroscopy is a simple, fast, and efficient technique for compound identification from complex materials [77].

SZ phyto-nanocarrier preparation was investigated using FT-IR spectroscopy to identify the presence of functional groups of both components (herb and clinoptilolite) (Table 3). FT-IR spectra of each constituent are shown in Figure 4.

Table 3. The characteristic absorption bands attributed to the phytoconstituents from *Sideritis scardica*.

Phytoconstituent	Wavenumber (cm ⁻¹)	Ref.
terpenoids	2940, 1745, 1700, 1650, 810	[78,79]
phenylethanoid glycosides	3390, 2853, 2925, 1720, 1700, 1628, 1602, 1520, 1454, 1385, 1280	[80–82]
fatty acids	3600, 3020–3010, 2960, 2925, 2875, 2850, 2560, 1702, 1350, 1245, 724	[83–85]
flavonoids	4000–3124, 3140–2980, 1655, 1644, 1620, 1585, 1496, 1465, 1415, 1370, 1275, 1080, 770, 535	[86]
phenolic acids	1800–1650, 1730, 1640, 1625, 1518, 1440, 1412, 1365, 1310, 1260, 1165, 1090, 945, 805	[79,87]
iridoids	1740–1458, 1377, 1221–914	[88]
phytosterols	3425, 3350, 2935, 2832, 1752, 1642, 1465, 1385, 1190, 1065, 990, 950, 880, 741	[89,90]
amino acids	3400; 3330–3130; 2985, 2360–2530, 2130; 1725–1755 1690, 1675, 1665, 1650, 1645, 1630, 1625, 1610, 1500–1600	[91]
nucleoside	3350, 3105, 2925, 2800, 1670, 1470, 1395, 1270, 1210, 1140. 1095, 1055, 980, 905, 830, 770, 570, 450	[92]

**Figure 4.** FT-IR spectra of ironwort, clinoptilolite, and SZ phyto-nanocarrier system.

FT-IR spectrum of clinoptilolite (Figure 4) displays the vibrational bands characteristic at 3630 cm⁻¹ (attributed to Si–O(H)–Al), 1645 cm⁻¹ (H–O–H deformation vibration), 1230 cm⁻¹ (associated with Si (Al)–O asymmetric stretching vibration) 1060 and 795 cm⁻¹ (associated to Si–O stretching vibration), 605 cm⁻¹ (corresponding to Si–O–Al and Si–O–Si bending vibrations), 554 cm⁻¹ (assigned to Si–O–Si symmetric stretching vibration and O–Si–O bending vibration), and 470 cm⁻¹ (assigned to Si–O–Si vibrational deformation) [93–95].

The FT-IR spectra of the SZ phyto-nanocarrier (Figure 4) include all the characteristic peaks of ironwort (at 3383 cm⁻¹ (-OH group), 2880 (C–H), 1745 (cyclopentanone ring of iridoids), 1706 (carboxyl acid C=O stretching), 1630 (COO- stretching vibration), 1644 (N–H of amino acids), 1385 cm⁻¹ (C–H bending), 1242 and 1015 (C–N of amine), 880 and 817 cm⁻¹ (C–O and CH vibration of aromatic rings), as well the clinoptilolite vibrational bands. However, several changes are detectable in the intensity of bands in the C–O, C–H, and N–H regions (1573, 1382, 1250, 1205 cm⁻¹). In addition, the absorption bands characteristic to clinoptilolite at 554 (Si–O–Si) and 795 cm⁻¹ (Si–O–Si and O–Si–O) are shifting to lower wavenumbers indicating that this functional group is involved in SZ phyto-nanocarrier formation.

2.4.2. X-ray-Diffraction Spectroscopy

X-ray-diffraction spectroscopy (XRD) is a rapid, routine, cost-effective analytic method used to obtain information on the atomic structure of a material and phase identification [96].

The XRD patterns of SZ phyto-nanocarrier, ironwort, and clinoptilolite are shown in Figure 5.

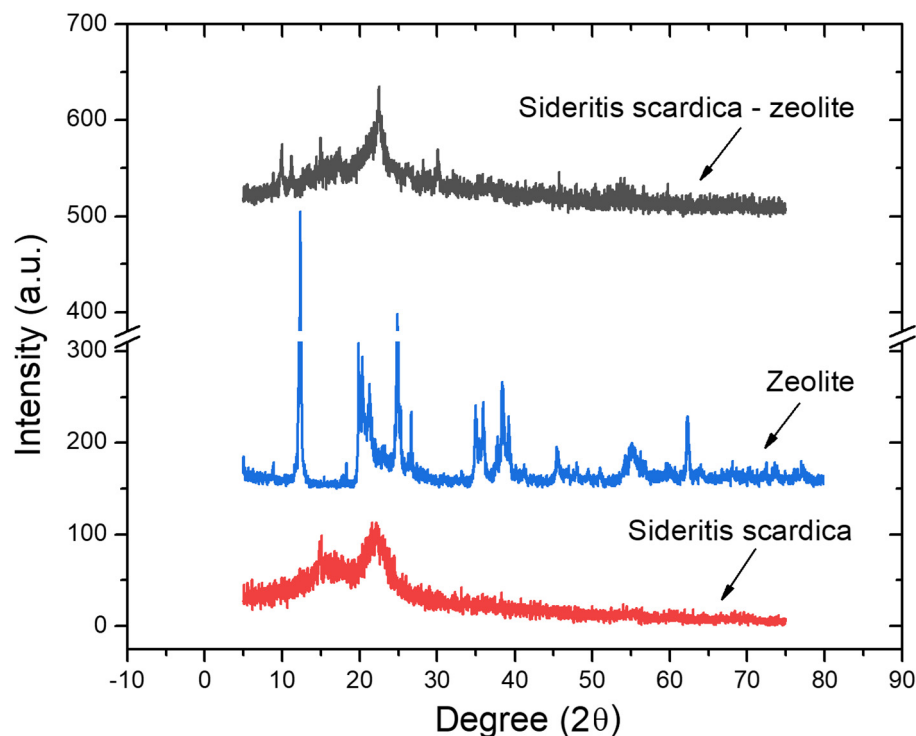


Figure 5. Powder XRD patterns of ironwort, clinoptilolite, and SZ phyto-nanocarrier.

Clinoptilolite presents diffraction peaks (at 2θ : 11.15° , 17.28° , 22.17° , 22.38° , 23.54° , 24.19° , 26.18° , and 33.39°) of crystalline phase of clinoptilolite zeolite structure with a crystallite mean size of 31.9 nm calculated using Scherrer equation (Figure 5) [97,98].

The corresponding spectrum of ironwort (Figure 5) displays large bands and weak diffraction peaks (in the range of 14.9 – 31.23°) characteristic of amorphous phases that can be assigned to different minerals and fibers from ironwort [99].

In the XRD pattern of the SZ phyto-nanocarrier are visible the diffraction peaks from both components (clinoptilolite and ironwort) are nonetheless significantly attenuated. Moreover, the characteristics peaks of clinoptilolite (at 2θ : 11.15° , 17.28° , 22.17° , and 22.38°) are shifted to lower angles that suggest the expansion of the zeolite lattice due to the loading of herbs particles [100].

The XRD results confirm that the new phyto-nanocarrier was effectively achieved.

2.4.3. Scanning Electron Microscopy (SEM)

Scanning Electron Microscopy (SEM) is a versatile analytical technique used currently to provide insight into surface topography and details on the sample structure.

Figure 6 shows the SEM micrograph of ironwort, clinoptilolite, and SZ phyto-nanocarrier.

The SEM image of the herb component (Figure 6A) depicts a fibrous surface and porous area alongside several particles of nanometric sizes and irregular shapes. The clinoptilolite micrograph (Figure 6B) exhibits a cluster of cubic and orthogonal nano-sized particles (average size ~ 30 nm), thus confirming the XDR results.

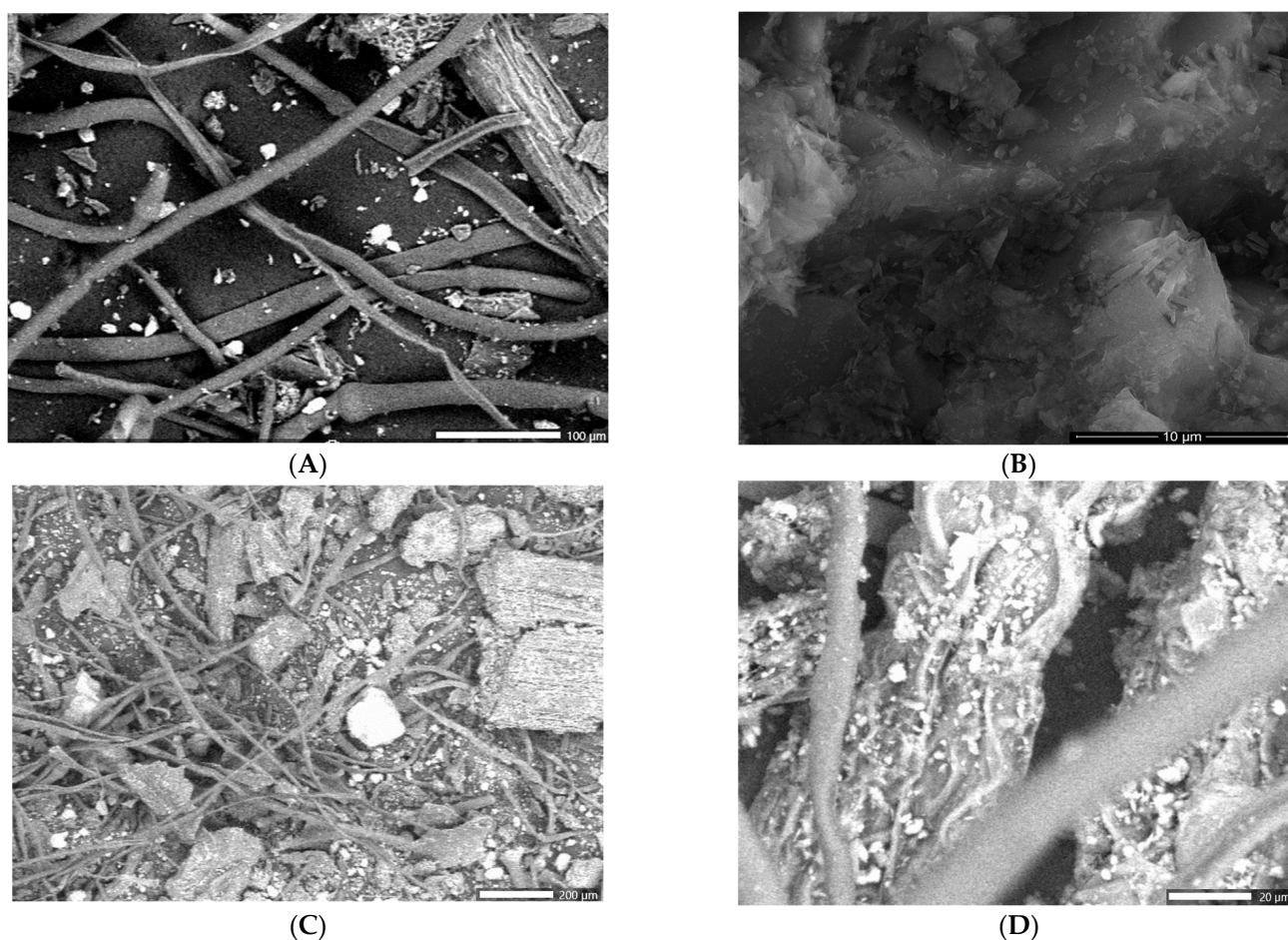


Figure 6. SEM images of ironwort (A), clinoptilolite (B), and SZ phyto-nanocarrier (C,D).

The SZ phyto-nanocarrier micrograph (Figure 6C,D) indicates the presence of agglomeration of nanoparticles from herb loaded into clinoptilolite pores and fibrous structures adhering to the surface of the clinoptilolite nanoparticles, probably due to electrostatic interaction. Additionally, it appears that clinoptilolite nanoparticles are loaded into fibrous structures, presumably due to the mechanical forces under employed experimental conditions. On the other hand, SEM indicates a size decrease for both component particles according to the phyto-nanocarrier experimental preparation procedure [101].

2.4.4. Energy Dispersive X-ray (EDX)

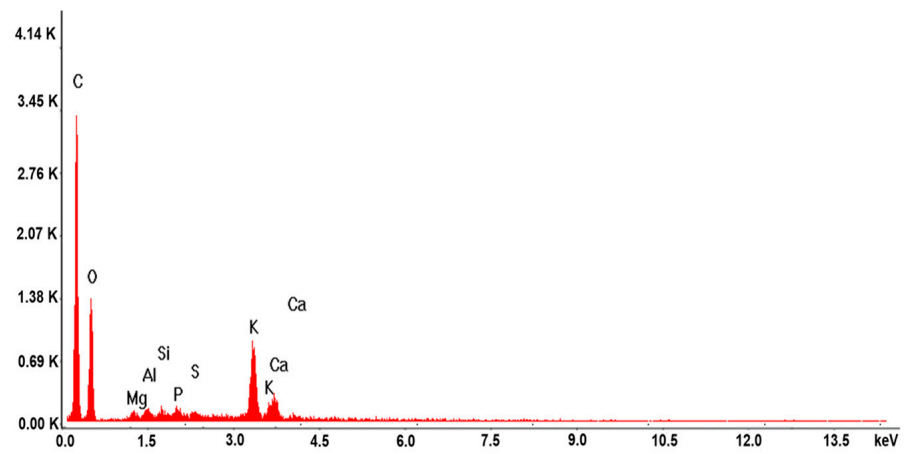
The elemental composition of all samples were investigated using (Energy Dispersive X-ray) technique (Figure 7).

According to the EDX spectra (Figure 7B), the clinoptilolite sample is composed of Si (32.31%), Al (7.44%), O (52.43%), K (3.17%), Ca (2.33%), and Fe (0.62%), corroborating the data reported in the literature [102].

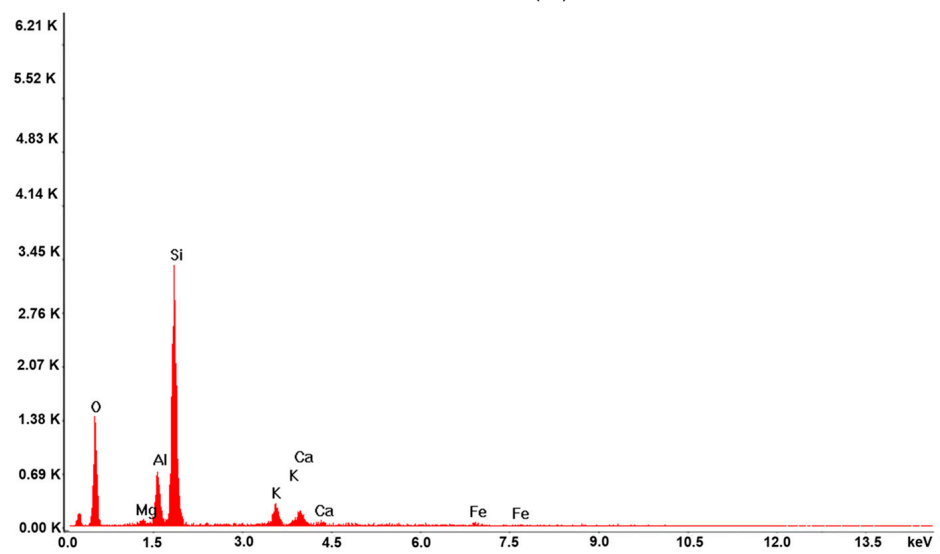
The SZ phyto-nanocarrier EDX spectra (Figure 7C) exhibit the peaks corresponding to ironwort (Figure 7A) and clinoptilolite samples, confirming their successful preparation.

2.5. Dynamic Light Scattering (DLS)

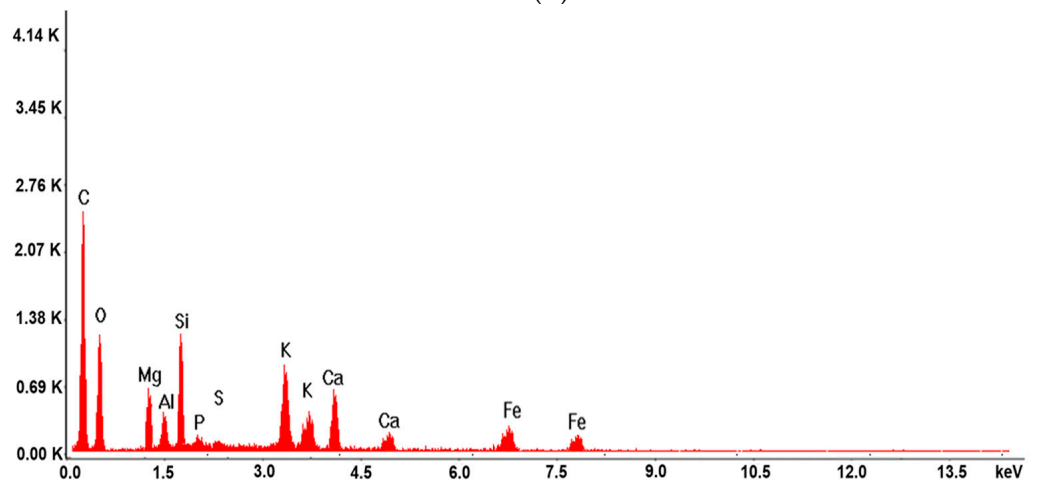
The stability and dynamics of the newly prepared phyto-nanocarrier were evaluated using DLS analysis. The average mean particle size (Table 4) and distribution profile of all samples (Figure 8) were studied using the DLS method.



(A)



(B)

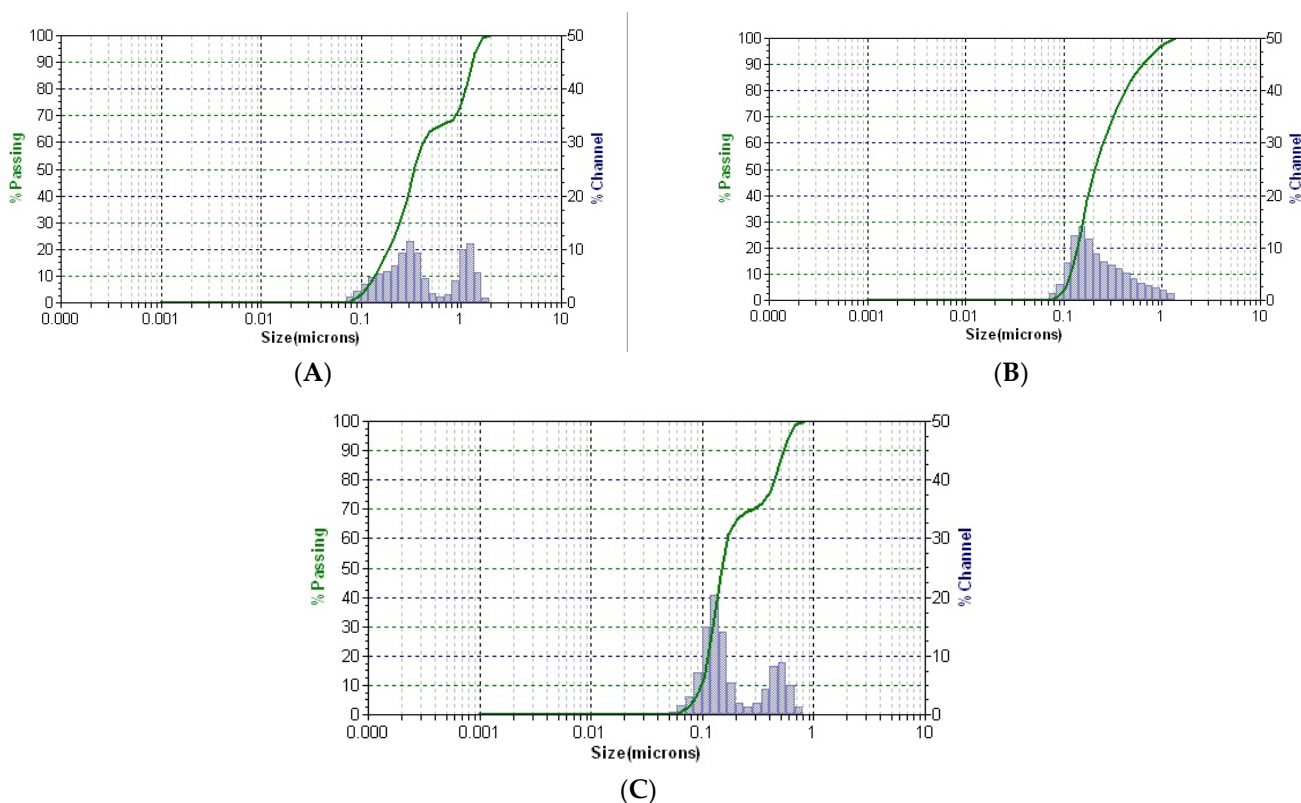


(C)

Figure 7. EDX composition of ironwort (A), clinoptilolite (B), and SZ phyto-nanocarrier (C).

Table 4. The DLS mean hydrodynamic diameter values of the SZ phyto-nanocarrier and both components.

Sample	Diameters (μm)	Width (μm)
ironwort	1.1710	0.4540
	0.2609	0.2383
clinoptilolite	0.2052	0.3530
SZ phyto-nanocarrier	0.4880	0.2170
	0.1299	0.0637

**Figure 8.** DLS patterns of ironwort (A), clinoptilolite (B), and SZ phyto-nanocarrier (C).

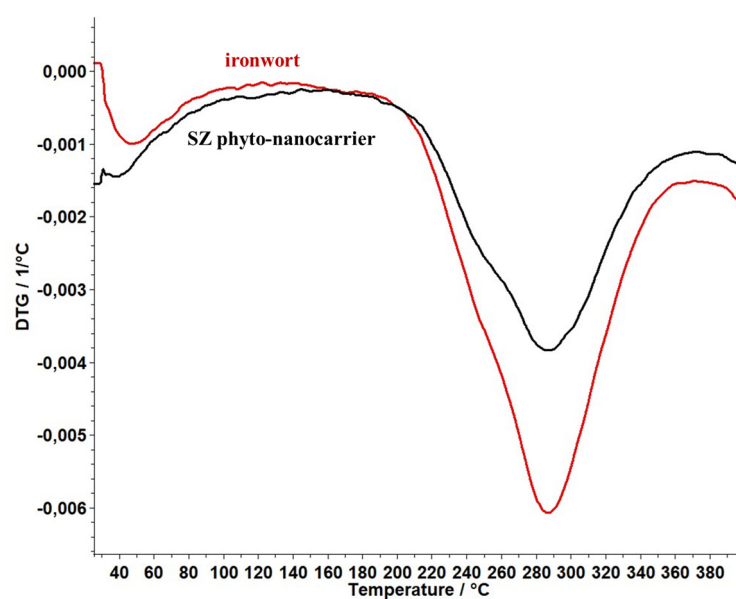
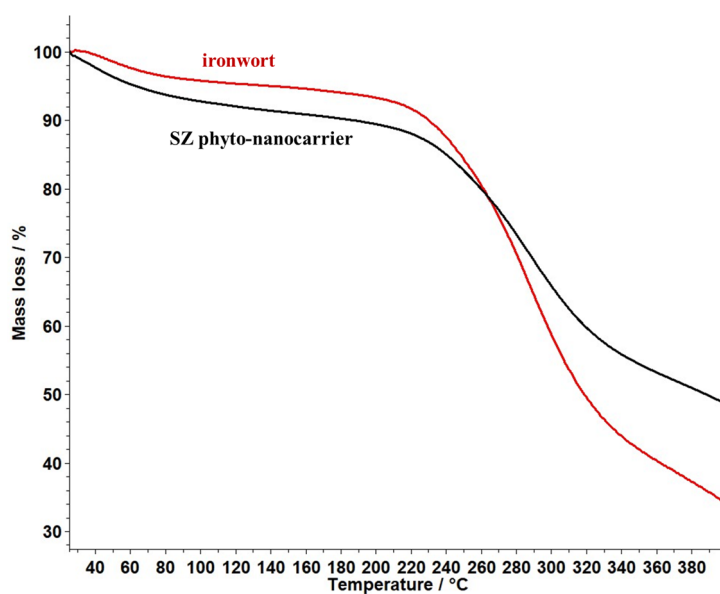
The dynamic light scattering (DLS) analysis conducted on the ironwort sample (Figure 8A) revealed two distinct peaks attributed to fibrous structures and herb particle presence, with different hydrodynamic diameter values (as indicated in Table 5). Similarly, the DLS pattern of the SZ phyto-nanocarrier (Figure 8C) also exhibited two distinct peaks, which suggested the presence of herb particles (with a diameter size of 130 nm) and clinoptilolite particles (measuring approximately 488 nm). Remarkably, the average diameter of herb particles in the phyto-carrier was significantly lower than that in the herb sample. This difference could be attributed to the experimental procedure employed for phyto-nanocarrier preparation that perhaps led to changes in surface electric charge, which consequently influenced the sample dispersibility and hydrodynamic diameter. Furthermore, the change in size of the clinoptilolite particles from the composition of the phyto-nanocarrier relative to the initial clinoptilolite sample indicated the loading of the pores with plant particles, confirmed by the SEM analysis results. Additionally, Figure 8C indicated that both components were well-dispersed into a narrow range, indicating that the SZ phyto-nanocarrier exhibited high stability. Overall, the DLS analysis provided valuable insights into the properties of the samples, which can be used to devise better experimental protocols for future studies.

Table 5. The results of phenolic contents, total antioxidant capacity, and IC₅₀ values for ironwort and SZ phyto-nanocarrier.

Sample Name	Total Phenolic Content (mg/g GAE)	mg AAE/mL	IC ₅₀ (mg/mL)
ironwort	0.4988 ± 0.072	122.23 ± 0.015	4.17 ± 0.019
SZ phyto-nanocarrier	0.5219 ± 0.010	165.37 ± 0.023	3.89 ± 0.034

2.6. Thermal Behaviour Study

The thermogravimetric analysis (TG) and differential thermogravimetric analysis (DTG) methods were used to investigate the physical and chemical changes of ironwort and SZ phyto-nanocarrier as a function of temperature. The results are shown in Figures 9 and 10.

**Figure 9.** DTG thermograms ironwort sample and SZ phyto-nanocarrier.**Figure 10.** TG thermograms of ironwort sample and SZ phyto-nanocarrier.

The profile of the thermogravimetric curve (Figure 10) indicates the presence of an endothermic process in the case of both investigated compounds.

According to Figure 9, ironwort displays one important weight loss (53%) in the temperature range of 200–367 °C associated with moisture loss, decarboxylation of volatile compounds, decomposition of phenolics, amino acids, carbohydrates, and polysaccharides [103,104].

The data for the SZ phyto-nanocarrier (Figure 9) exhibited a weight loss (35%) in the temperature range of 200–355 °C attributed to herb biomolecules and, thus, an improvement in thermal stability compared to the ironwort sample.

2.7. Screening of Antioxidant Activity and Total Polyphenolic Contents

Considering the great diversity of biomolecules in the chemical composition of medicinal plants, the selection of assays for the antioxidant activity evaluation is required. The most common are chemical or biochemical methods for the total antioxidant activity potential directly estimated from plant matrices [105].

Among the most frequently used are the *in vitro* tests, divided into two large categories: methods based on the transfer of a hydrogen atom (HAT) or electron transfer (ET). For complex matrices, the most fashionable are the *in vitro*, non-competitive, non-enzymatic assays for the estimation of antioxidant activity based such as CUPRAC, DPPH, FRAP, ABTS, ABTS/TEAC, or others [106–109]. In view of the aforementioned grounds, selectivity, accuracy, low cost, and speed are the main criteria for selecting a specific assay [106–109].

The biological properties of the new phyto-nanocarriers are due to the conjugate and synergic action of the multiple phytoconstituents from the ironwort sample, which are complementary to the carrier (clinoptilolite). Hence, three distinct assays (DPPH, Total polyphenolic contents (Folin-Ciocalteu), and phosphomolybdate (total antioxidant capacity)) were chosen to obtain an accurate insight into the phyto-carrier antioxidant potential.

2.7.1. Total Polyphenolic Contents (TPCs) Assay—Folin Ciocalteu

The Folin–Ciocalteu assay is a recognizable *in vitro* method for polyphenol evaluation from plant extracts or other natural product derivatives.

The results of the TPCs assay obtained for the new phyto-nanocarrier and its components are presented in Table 5 and Figure 11A.

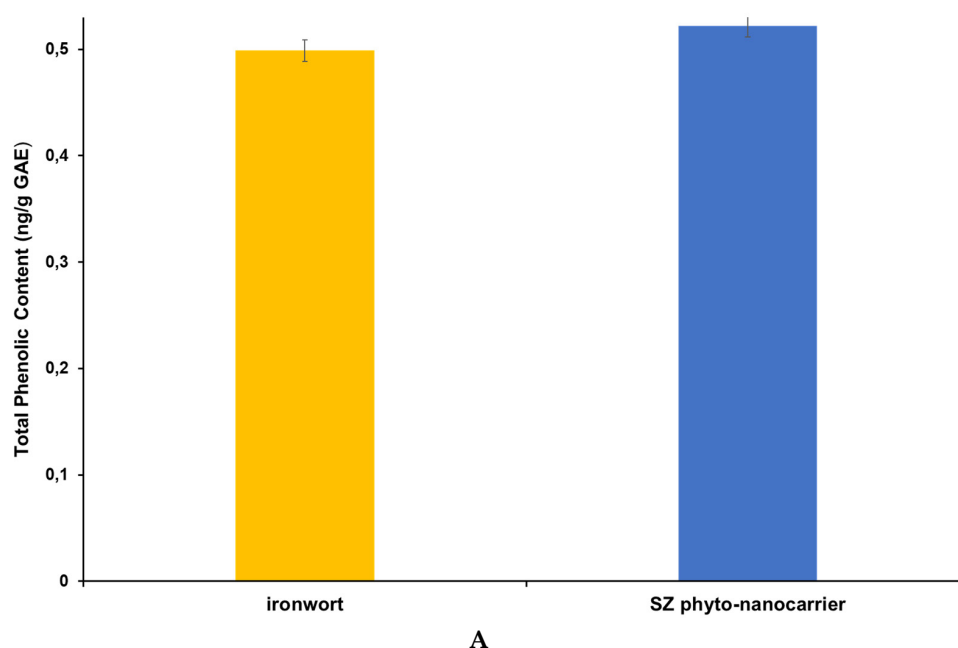


Figure 11. Cont.

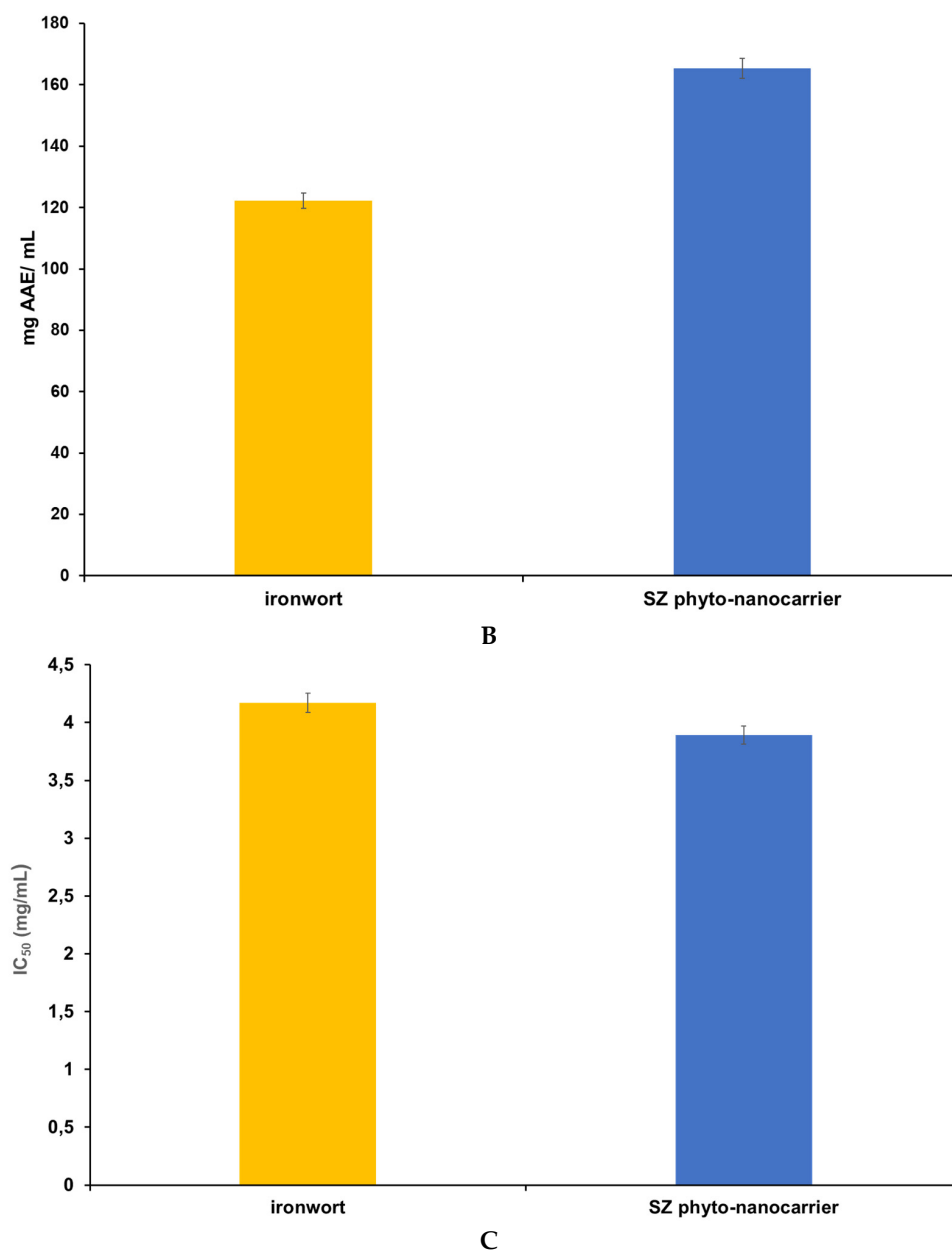


Figure 11. Graphic representation of Total Phenolic (A), Total Antioxidant Capacity (B), and DPPH (C) results.

According to the obtained data, a slight increase (about 4.65%) of total polyphenolic content of the SZ phyto-nanocarrier than the ironwort sample, indicating a synergistic action of clinoptilolite [11–14].

2.7.2. Phosphomolybdate Assay (Total Antioxidant Capacity)

Phosphomolybdate (total antioxidant capacity) is a classical, simple, and accurate technique used for total antioxidant capacity quantitative evaluation from a highly complex mixture of bioactive compounds [110].

Total antioxidant capacity was determined for SZ phyto-nanocarrier, and the data are shown in Table 5 and Figure 11B.

Based on the obtained results, the SZ-phyto-carrier phyto-nanocarrier system has higher antioxidant activity (about 35.3%) than that of the herb sample, suggesting that, under the employed experimental conditions, loading the plant in the clinoptilolite pores induces a favorable effect on antioxidant potential.

2.7.3. DPPH (1,1-diphenyl-2-picrylhydrazyl) Free-Radical-Scavenging Assay

2,2-diphenyl-1-picrylhydrazyl (DPPH) assay is a straightforward, specific, sensitive, fast technique for the free radical DPPH scavenging capacity assessment in various heterogeneous mixtures [109].

Results of DPPH for SZ phyto-nanocarrier and herb component are presented in Table 5 and Figure 11C.

According to the data, and given that lower IC_{50} values correspond to higher antioxidant activity, the SZ phyto-nanocarrier exhibits a slight increase (up to 7.2%) compared to the ironwort sample, might be due to the biomolecules loaded in clinoptilolite pores, which is in good agreement with the literature [11–14].

The collective results of the antioxidant assays used in this study indicate that the new phyto-nanocarrier prepared has a very high antioxidant activity compared to the plant sample, considering the influence of the reaction parameters (molar ratio, solvent polarity, pH, temperature) such as and the modification of the structural properties (size particles, specific surface, etc.) occurring as a result of the employed experimental procedure [111,112]. Various studies reported that loading the zeolite pores with phytochemicals enhances *in vivo* biocompatibility and stability, as well as prolonged controlled release [18,19].

2.8. *In Vitro* Dissolution Assay

In vitro, dissolution testing is extensively used as a significant technique to evaluate *in vivo* performance in the digestive tract and, implicitly, their bioavailability and therapeutic efficiency.

Herbal preparations contain numerous phytoconstituents (belonging to distinct chemical categories) in various proportions depending on different biotic and abiotic parameters (including the selected extraction procedures), which determines variations in adsorption properties and pharmacological effectiveness [113–118]. Consequently, *in vivo*, biopharmaceutical performance mimic and prediction for natural products is far more challenging than single-component synthetic drugs [119–121].

The physiological pH in the human digestive tract varies from 1.2 to 7.8. Hence, the appropriate dissolution environment provides valuable information on absorption properties. Commonly, in aqueous media, small amounts of various surfactant types are added to promote the solubility of some phytoconstituents.

The dissolution profile of ironwort and SZ phyto-nanocarrier at two different pH values (pH 4 and pH 7) were investigated as a function of time [117,118].

To that end, the relationship between pH and dissolution rates is shown in Figure 12.

The results indicate that both samples had increased dissolution time in an acidic environment (pH 4) over time. Although both samples exhibited a relatively similar dissolution profile, it can be observed that the SZ phyto-nanocarrier performed better, displaying a dissolution of about 25% until 120 min, compared to the ironwort sample. Subsequently, this difference decreased to approximately 15% (Figure 12). Both samples demonstrated a high degree of rapid release within 30 min, about 75% for ironwort and about 85% for SZ phyto-nanocarrier, reaching a maximum of 96.37% for ironwort and 99.76% for SZ phyto-nanocarrier at 60 min (Figure 12A,C). These results are in good agreement with the requirements imposed by international regulations [116].

The dissolution rate showed a notable shift with the pH modification. At pH 7, the release rate was still fast, about 72% for ironwort and 80% for SZ phyto-nanocarrier, but slightly lower than at pH 4 (Figure 12A,C). The results indicate that the maximum release was reached at 150 min for both samples, 94% for ironwort and 99% for SZ phyto-nanocarrier (Figure 12A,C).

Recent literature results have reported that the bioavailability of a drug depends on various physical characteristics of drug delivery, such as particle size, shape, and long-range structural (atomic-scale) order [117,118].

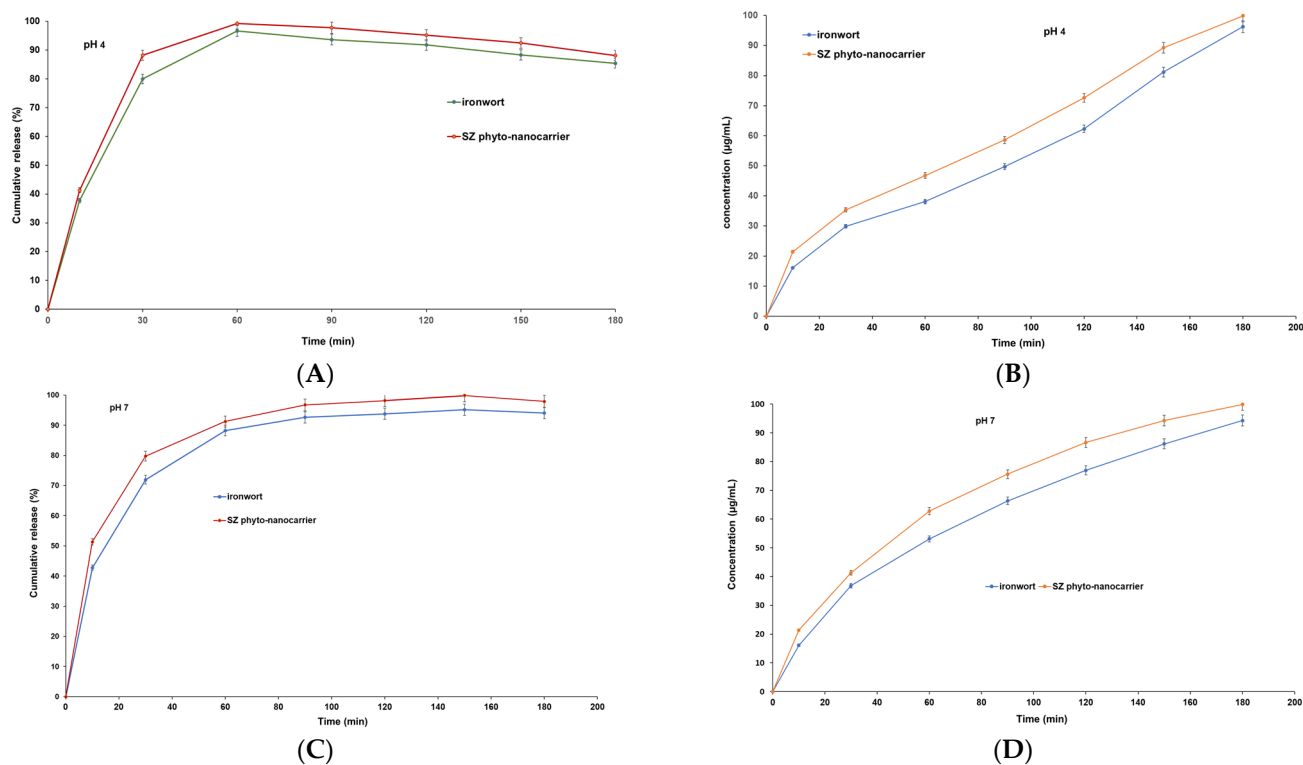


Figure 12. Dissolution profile of ironwort and SZ phyto-nanocarrier.

Therefore, the enhanced dissolution rate of the SZ phyto-nanocarrier can be attributed to the reduction in particle size and increased specific surface area under the employed experimental conditions. Furthermore, the variation of the dissolution speed with the pH value suggests the formation of electrostatic or van der Waals interactions. In an acid medium (pH = 4), both investigated compounds (ironwort and SZ phyto-nanocarrier) demonstrated a higher dissolution rate than the value obtained at pH = 7, indicating that it is most suitable for adsorption. These findings provide valuable insights into the potential applications of SZ phyto-nanocarrier in the pharmaceutical and nutraceutical industries.

3. Materials and Methods

3.1. Reagents and materials

All reagents used in this study were of analytical grade, acquired from commercial suppliers, and used without further purification. Methanol, ethanol, dichloromethane, chloroform, gallic acid, ascorbic acid, 2,2-diphenyl-1-picrylhydrazyl, sodium phosphate, potassium chloride (99% were also purchased from), anhydrous sodium carbonate, potassium persulfate, ammonium molybdate, and Folin–Ciocalteu phenol reagent (2 N) were purchased from Sigma-Aldrich (München, Germany). Buffer solution pH 7 (di-sodium hydrogen phosphate/potassium dihydrogen phosphate), Buffer solution pH 4 (citric acid/sodium hydroxide/hydrogen chloride) (Merck Millipore (Darmstadt, Germany). Ultrapure water was used in all experiments.

Clinoptilolite samples (Baia Mare, Romania, were offered by the University Politehnica Timisoara (Timisoara, Romania). It was micronized using a planetary mill Fritsch Pulverisette mill (Idar-Oberstein, Germany) (500 rpm for 20 min at 23 °C) and then sieved through several ASTM sieves. The present study made use only of particle size within the range of 1.3–3.0 µm. Subsequently, the clinoptilolite sample was washed with ultrapure water, dried at 100 °C, and then stored in a desiccator [95].

Sideritis scardica Griseb. (ironwort) samples (dried stems, leaves, and flowers) were provided by the University of Medicine and Pharmacy Craiova, Romania.

3.2. Plant Samples' Preparation for Chemical Screening

The ironwort samples were milled using a planetary mill, sieved to obtain particle diameters ranging from 0.25–0.30 mm, and then stored until further use. The ultrasonic-assisted extraction was carried out using (1.5 g dried plant sample: 20 mL solvent) a methanol/chloroform mixture (1:1, *v/v*) at 35 °C and 60 Hz for 30 min (Elmasonic, Singen, Germany). Then, the solvent mixture was removed using a rotary evaporator (Rotavapor; BÜCHI, Flawil, Switzerland) at 30 °C. The residue obtained was dissolved with MeOH (15 mL), centrifuged, and then filtered (0.20 µm) and stored at –30 °C. All experiments were prepared in triplicate.

3.2.1. GC-MS Analysis (EZ: Faast GC-MS Free Amino Acids Kit)

Gas chromatography was carried out using a GCMS-QP2020NX Shimadzu apparatus (Shimadzu, Kyoto, Japan) with a ZB-5MS capillary column (30 m × 0.25 mm id × 0.25 µm) (Phenomenex, Torrance, CA, USA), helium (flow rate of 1 mL/min).

GC-MS Separation Conditions

The oven temperature was increased from 50 °C (kept for 2 min) to 300 °C (rate of 5 °C/min, kept for 5 min). The temperature of the injector was 300 °C, and the temperature at the interface was 215 °C. The mass of the compounds was registered at a 70 eV ionization energy. The mass spectrometer was source-heated at 220 °C, and the MS Quad was heated at 150 °C. The results obtained are shown in Table 1.

3.2.2. Mass Spectrometry

The MS experiments were performed using an EIS-QTOF-MS (Bruker Daltonics, Bremen, Germany). The mass spectra were acquired in the positive ion mode in a mass range of 70–3000 *m/z*. The scan speed was 2.2 scans/s, the collision energy was 10–85 eV, and the temperature of the source block was 80 °C [38,51,79,99].

Compounds were identified based on their mass spectra, which were compared to the NIST 3.0 database mass spectra library database (USA National Institute of Science and Technology software) (NIST, Gaithersburg, MD, USA) and literature review. The biomolecules identified are presented in Table 2.

3.3. SZ Phyto-Nanocarrier

To prepare the SZ phyto-nanocarrier, the ironwort sample (dried herb) and clinoptilolite were added (1:2.5 mass ratio), then ground, and homogenized for 10 min using planetary mill Fritsch Pulverisette mill. Each experiment was repeated three times.

3.4. Characterization of Phyto-Nanocarrier and Its Components

3.4.1. Fourier Transform Infrared (FT-IR) Spectroscopy

FT-IR spectra of SZ phyto-nanocarrier, ironwort, and clinoptilolite were recorded (range of 400–4000 cm⁻¹, resolution of 4 cm⁻¹) on a Fourier transform infrared spectrometer (Shimadzu AIM-9000 with ATR devices).

3.4.2. XRD Spectroscopy

The phase composition of the phyto-nanocarrier and each component were investigated using a Bruker AXS D8-Advance X-ray diffractometer (Bruker AXS GmbH, Karlsruhe, Germany) equipped with a rotating sample stage, Anton Paar TTK low-temperature cell (–180–450 °C), high-vacuum, inert atmosphere, relative humidity control. The average crystallite size and the phase content were determined using the whole-pattern profile-fitting method (WPPF).

3.4.3. Scanning Electron Microscopy (SEM)

Morpho-structural analysis was conducted on a SEM-EDS system (JEOL JSM-IT200 Field Emission, Nieuw-Vennep, The Netherlands) equipped with a high-resolution electron gun and energy-dispersive X-ray spectrometer (EDS).

3.4.4. Dynamic Light Scattering (DLS) Particle Size Distribution Analysis

The DLS analysis was performed on a scattering angle of 172° at room temperature (23 °C) using a Microtrac/Nanotrak 252 (Montgomeryville, PA, USA) instrument. Each experiment was repeated three times.

3.5. Thermal Analysis

The thermal stability of the SZ phyto-nanocarrier and ironwort sample was studied in a dynamic air atmosphere (20 mL/min, synthetic air) at the temperature range (25 and 400 °C), with a 10°/min heating rate) using a Thermal Analyzer produced by Mettler Toledo, model TGA/DSC3+ STARe System. The DSC analysis was performed in an air atmosphere (50 mL/min) with a temperature range (25–400 °C) on a DSC 3+ Mettler Toledo.

3.6. Antioxidant Activity and Total Phenolic Content

The antioxidant potential of SZ phyto-nanocarrier and its components were estimated employing three different assays: total phenolic content (Folin–Ciocalteu) assay, 2,2-diphenyl-1-picrylhydrazyl (DPPH) radical scavenging assay and phosphomolybdate assay (total antioxidant capacity). The experimental procedure was the following: Round-bottom flasks (50 mL) containing 0.20 (±0.001) g solid sample to which 10 mL ethanol (70%) was added. Subsequently, the mixture was subjected to sonication extraction for 30 min, 200 rpm, at 45 °C. Extracted solutions were centrifuged at 3500 rpm for 10 min, and then the supernatant was collected for use in the selected antioxidant assays for this study.

3.6.1. Total Polyphenol Content Using the Folin–Ciocalteu Method

The total phenolic content in SZ phyto-nanocarrier and its components were determined using a UV-VIS spectrophotometry (DLAB SP-UV1000, Penjuru, Singapore), according to the Folin–Ciocalteu experimental procedure adapted from the literature [122].

The sample extract concentrations were calculated based on the linear equation obtained from the standard curve ($y = 0.0028x + 0.0264$ and the correlation coefficient ($R^2 = 0.9967$)).

3.6.2. DPPH Radical Scavenging Assay

The antioxidant activities of SZ phyto-nanocarrier and ironwort samples were comparatively investigated using a DPPH (2,2-diphenyl-1-picrylhydrazyl) free radical elimination assay. The extract samples were prepared at different concentrations in the range of 0.020 and 20 mg/mL. Then, 1.5 mL of DPPH working solution was transferred to all sample extracts (10 µL), mixed, and left in the dark for 30 min. All analyses were carried out in triplicates, and absorbance was recorded at 510 nm. The results were used to determine the inhibition percentage (Inh%) according to Equation (1).

$$\text{Inh\%} = (A_0 - A_1)/A_0 \times 10 \quad (1)$$

The IC₅₀ (half-maximal inhibitory concentration) values were obtained from the inhibition percentage using the equation from the calibration curve generated for each sample.

3.6.3. Phosphomolybdate Assay (Total Antioxidant Capacity)

The total antioxidant capacity assay of SZ phyto-nanocarrier and ironwort sample was carried out according to phosphomolybdenum, a procedure described in our earlier publication [111]. The results are presented as µg/mL of ascorbic acid equivalents (AAE).

3.7. In Vitro Dissolution Test

Dissolution profiles of ironwort ($0.5 \text{ g} \pm 0.045$) and SZ phyto-nanocarrier ($0.5 \text{ g} \pm 0.019$) were determined using a 708-DS Dissolution -Agilent Technologies (Santa Clara, CA, USA) at $37 \pm 0.5 \text{ }^\circ\text{C}$, 100 rpm in 600 mL of two buffers of distinct pH value: pH 4 (simulated the stomach fluids) and pH 7 (simulated the intestinal fluids) and sink conditions were maintained throughout the dissolution rate tests [123].

The evaluation of dissolution profiles was carried out at 15, 30, 45, 60, 90, and 120 min.

A total of 15 mL of an aliquot of the dissolution medium was automatically collected at the set time interval and filtrated ($0.45 \text{ }\mu\text{m}$). The cumulative drug released against time was determined using a UV-Vis Perkin-Elmer Lambda 35 (Perkin Elmer, Waltham, MA, USA) [123].

Triplicate samples were analyzed at each time. The mean value of six samples and a standard deviation were calculated [124].

Preparation of the Curves of the Concentrations for the Compound Dissolution Profile

Different solution concentrations (in the range of 0.001 and 0.25 mg/mL) were prepared from each compound (ironwort and SZ phyto-nanocarrier, respectively). Calibration curves were plotted for ironwort and SZ phyto-nanocarrier. The amount of each compound released was obtained from the standard curve of the concentration versus its absorbency. The correlation coefficients, at pH = 4 were: $R^2 = 0.9987$ (ironwort) and $R^2 = 0.9978$ (SZ phyto-nanocarrier); at pH = 7, $R^2 = 0.9989$ (ironwort) and $R^2 = 0.9973$ (SZ phyto-nanocarrier) demonstrate the good linear relationship of the data.

The compound release was calculated according to the following equation [125]

$$\text{CDR}(\%) = \frac{\text{amount of released compound at time } n \text{ (g)}}{\text{amount compound used as raw materials (g)}} \times 100 \quad (2)$$

3.8. Statistical Analysis

Each experimental set was performed in triplicate, using one-way analysis of variance (ANOVA) without replication with Scheffe's post hoc test comparison; $p < 0.05$ was taken as statistically significant. Data are presented as the means \pm SD.

4. Conclusions

This study presents the preparation and a comprehensive evaluation conducted to assess the potential of a newly developed nanocarrier derived from *Sideritis scardica* Griseb and clinoptilolite. The unique features of the new nanocarrier were confirmed through various analytical methods (FT-IR, XRD, SEM-EDX, DLS).

Accordingly, the reduction in particle size and specific surface area increases due to loading the herb into clinoptilolite pores, allowing better thermal stability and an increase in antioxidant potential and dissolution rate compared to the herb sample. Based on the results, the nanocarrier shows great promise as a candidate for drug delivery systems. However, further research is needed to explore its potential biomedical applications.

Author Contributions: Conceptualization, A.-E.S.; methodology, A.-E.S.; formal analysis, G.V., T.V., A.B., G.B. and A.D.; investigation, G.V., T.V., A.B., C.B., G.B., L.E.B. and E.R.B.; writing—review and editing, A.-E.S. All authors have read and agreed to the published version of the manuscript.

Funding: This research received no external funding.

Institutional Review Board Statement: Not applicable.

Informed Consent Statement: Not applicable.

Data Availability Statement: Data is contained within the article.

Conflicts of Interest: The authors declare no conflicts of interest.

References

1. Ververis, A.; Ioannou, K.; Kyriakou, S.; Violaki, N.; Panayiotidis, M.I.; Plioukas, M.; Christodoulou, K. *Sideritis scardica* extracts demonstrate neuroprotective activity against A β _{25–35} toxicity. *Plants* **2023**, *12*, 1716. [[CrossRef](#)]
2. Aneva, I.; Zhelev, P.; Kozuharova, E.; Danova, K.; Nabavi, S.F.; Behzad, S. Genus *Sideritis*, section *Empedoclia* in SouthEastern Europe and Turkey—Studies in ethnopharmacology and recent progress of biological activities. *DARU J. Pharm. Sci.* **2019**, *27*, 407–421. [[CrossRef](#)]
3. Moussavi, N.; Azizullah, H.; Malterud, K.E.; Inngjerdigen, K.T.; Wangensteen, H. Immunomodulating polyphenols from *Sideritis Scardica*. *J. Funct. Foods* **2022**, *96*, 105197. [[CrossRef](#)]
4. González-Burgos, E.; Carretero, M.E.; Gómez-Serranillos, M.P. *Sideritis* spp.: Uses, chemical composition and pharmacological activities—A review. *J. Ethnopharmacol.* **2011**, *135*, 209–225. [[CrossRef](#)] [[PubMed](#)]
5. Żyżelewicz, D.; Kulbat-Warycha, K.; Oracz, J.; Żyżelewicz, K. Polyphenols and other bioactive compounds of *Sideritis* plants and their potential biological activity. *Molecules* **2020**, *25*, 3763. [[CrossRef](#)]
6. Rahman, H.S.; Othman, H.H.; Hammadi, N.I.; Yeap, S.K.; Amin, K.M.; Abdul Samad, N.; Alitheen, N.B. Novel drug delivery systems for loading of natural plant extracts and their biomedical applications. *Int. J. Nanomed.* **2020**, *15*, 2439–2483. [[CrossRef](#)] [[PubMed](#)]
7. Atanasov, A.G.; Zotchev, S.B.; Dirsch, V.M.; Supuran, C.T. Natural products in drug discovery: Advances and opportunities. *Nat. Rev. Drug Discov.* **2021**, *20*, 200–216. [[CrossRef](#)]
8. Singh, I.P.; Ahmad, F.; Chatterjee, D.; Bajpai, R.; Sengar, N. Natural products: Drug discovery and development. In *Drug Discovery and Development from Targets and Molecules to Medicines*; Poduri, R., Ed.; Springer: Singapore, 2021; ISBN 978-981-15-5533-6.
9. Nath, R.; Roy, R.; Barai, G.; Bairagi, S.; Manna, S.; Chakraborty, R. Modern developments of nano based drug delivery system by combined with phytochemicals-presenting new aspects. *Int. J. Sci. Res. Sci. Technol.* **2021**, *8*, 107–129. [[CrossRef](#)]
10. Patra, J.K.; Das, G.; Fraceto, L.F.; Campos, E.V.R.; del Pilar Rodriguez-Torres, M.; Acosta-Torres, L.S.; Diaz-Torres, L.A.; Grillo, R.; Swamy, M.K.; Sharma, S.; et al. Nano based drug delivery systems: Recent developments and future prospects. *J. Nanobiotechnol.* **2018**, *16*, 71. [[CrossRef](#)] [[PubMed](#)]
11. Kraljević Pavelić, S.; Simović Medica, J.; Gumbarević, D.; Filošević, A.; Pržulj, N.; Pavelić, K. Critical review on zeolite clinoptilolite safety and medical applications *in vivo*. *Front. Pharmacol.* **2018**, *9*, 1350. [[CrossRef](#)]
12. Serati-Nouri, H.; Jafari, A.; Roshangar, L.; Dadashpour, M.; Pilehvar-Soltanahmadi, Y.; Zarghami, N. Biomedical applications of zeolite-based materials: A review. *Mater. Sci. Eng. C* **2020**, *116*, 111225. [[CrossRef](#)]
13. Mastinu, A.; Kumar, A.; Maccarinelli, G.; Bonini, S.A.; Premoli, M.; Aria, F.; Gianoncelli, A.; Memo, M. Zeolite clinoptilolite: Therapeutic virtues of an ancient mineral. *Molecules* **2019**, *24*, 1517. [[CrossRef](#)]
14. Souza, I.M.S.; García-Villén, F.; Viseras, C.; Pergher, S.B.C. Zeolites as ingredients of medicinal products. *Pharmaceutics* **2023**, *15*, 1352. [[CrossRef](#)] [[PubMed](#)]
15. Li, Y.; Cai, Y.; Chen, T.; Bao, X. Zeolites: A series of promising biomaterials in bone tissue engineering. *Front. Bioeng. Biotechnol.* **2022**, *10*, 1066552. [[CrossRef](#)]
16. Oggiano, G.; Pokimica, B.; Popovic, T.; Poštić, M. Beneficial properties of zeolite. *Ital. J. Food Sci.* **2023**, *35*, 72–78. [[CrossRef](#)]
17. Nikolov, A.; Dobreva, L.; Danova, S.; Miteva-Staleva, J.; Krumova, E.; Rashev, V.; Vilhelmova-Ilieva, N. Natural and modified zeolite clinoptilolite with antimicrobial properties: A review. *Acta Microbiol. Bulg.* **2023**, *39*, 147–161. [[CrossRef](#)]
18. Servatan, M.; Zarrintaj, P.; Mahmodi, G.; Kim, S.J.; Ganjali, M.R.; Saeb, M.R.; Mozafari, M. Zeolites in drug delivery: Progress, challenges and opportunities. *Drug Discov. Today* **2020**, *25*, 642–656. [[CrossRef](#)]
19. Ferreira, A.P.; Almeida-Aguiar, C.; Costa, S.P.G.; Neves, I.C. Essential oils encapsulated in zeolite structures as delivery systems (EODS): An overview. *Molecules* **2022**, *27*, 8525. [[CrossRef](#)]
20. Göktaş, S.; Ülkü, S.; Bayraktar, O. Clinoptilolite-rich mineral as a novel carrier for the active constituents present in Ginkgo biloba leaf extract. *Appl. Clay Sci.* **2008**, *40*, 6–14. [[CrossRef](#)]
21. Alsanad, S.; Howard, R.; Williamson, E. An assessment of the impact of herb-drug combinations used by cancer patients. *BMC Complement. Altern. Med.* **2016**, *16*, 393. [[CrossRef](#)] [[PubMed](#)]
22. Puri, V.; Nagpal, M.; Singh, I.; Singh, M.; Dhingra, G.A.; Huanbutta, K.; Dheer, D.; Sharma, A.; Sangnim, T.A. Comprehensive review on nutraceuticals: Therapy support and formulation challenges. *Nutrients* **2022**, *14*, 4637. [[CrossRef](#)]
23. Kiroğlu, O.; Berktaş, F.; Khan, Z.; Dağkiran, M.; Karatas, Y. Self-medication practices with conventional and herbal drugs among ear, nose, and throat patients. *Rev. Assoc. Médica Bras.* **2022**, *68*, 1416–1422. [[CrossRef](#)]
24. Sánchez, M.; González-Burgos, E.; Iglesias, I.; Lozano, R.; Gómez-Serranillos, M.P. Current uses and knowledge of medicinal plants in the autonomous community of Madrid (Spain): A descriptive cross-sectional study. *BMC Complement. Med. Ther.* **2020**, *20*, 306. [[CrossRef](#)]
25. Pal, S.K.; Shukla, Y. Herbal medicine: Current status and the future. *Asian Pac. J. Cancer Prev.* **2003**, *4*, 281–288.
26. Alam, S.; Sarker, M.R.; Afrin, S.; Richi, F.T.; Zhao, C.; Zhou, J.-R.; Mohamed, I.N. Traditional herbal medicines, bioactive metabolites, and plant products against COVID-19: Update on clinical trials and mechanism of actions. *Front. Pharmacol.* **2021**, *12*, 671498. [[CrossRef](#)] [[PubMed](#)]
27. Isah, T. Stress and defense responses in plant secondary metabolites production. *Biol. Res.* **2019**, *52*, 39. [[CrossRef](#)] [[PubMed](#)]
28. Yang, L.; Wen, K.-S.; Ruan, X.; Zhao, Y.X.; Wei, F.; Wang, Q. Response of plant secondary metabolites to environmental factors. *Molecules* **2018**, *23*, 762. [[CrossRef](#)] [[PubMed](#)]

29. Xie, P.; Wang, Y.; Wei, D.; Zhang, L.; Zhang, B.; Xiao, H.; Song, H.; Mao, X. Nanoparticle-based drug delivery systems with platinum drugs for overcoming cancer drug resistance. *J. Mater. Chem. B* **2021**, *9*, 5173–5194. [CrossRef] [PubMed]
30. Chiangjong, W.; Chutipongtanate, S.; Hongeng, S. Anticancer peptide: Physicochemical property, functional aspect and trend in clinical application (Review). *Int. J. Oncol.* **2020**, *57*, 678–696. [CrossRef] [PubMed]
31. Emran, T.B.; Shahriar, A.; Mahmud, A.R.; Rahman, T.; Abir, M.H.; Siddiquee, M.; Ahmed, H.; Rahman, N.; Nainu, F.; Wahyudin, E.; et al. Multidrug resistance in cancer: Understanding molecular mechanisms, immunoprevention and therapeutic approaches. *Front. Oncol.* **2022**, *12*, 891652. [CrossRef]
32. Ahmad, R.; Srivastava, S.; Ghosh, S.; Khare, S.K. Phytochemical delivery through nanocarriers: A review. *Colloids Surf. B Biointerfaces* **2021**, *197*, 111389. [CrossRef]
33. David J Newman, Natural products and drug discovery. *Natl. Sci. Rev.* **2022**, *9*, nwac206. [CrossRef] [PubMed]
34. Choudhury, F.K.; Pandey, P.; Meitei, R.; Cardona, D.; Gujar, A.C.; Shulaev, V. GC-MS/MS Profiling of Plant Metabolites. In *Plant Metabolic Engineering; Methods in Molecular Biology*; Shulaev, V., Ed.; Humana: New York, NY, USA, 2022; Volume 2396.
35. Proestos, C.; Sereli, D.; Komaitis, M. Determination of phenolic compounds in aromatic plants by RP-HPLC and GC-MS. *Food Chem.* **2006**, *95*, 44–52. [CrossRef]
36. Phenomenex, E.Z. Faast-Easy Fast Amino Acid Sampling Testing Kit-User Guide; Torrance, CA, USA 411 Madrid Avenue, Torrance, CA90501-1430, USA. Available online: <http://www.phenomenex.com> (accessed on 24 June 2023).
37. Triikka, F.; Michailidou, S.; Makris, A.; Argiriou, A. Biochemical fingerprint of *Greek sideritis* spp.: Implications for potential drug discovery and advanced breeding strategies. *Med. Aromat. Plants* **2019**, *8*, 1–11. [CrossRef]
38. Segneanu, A.-E.; Grozescu, I.; Cziple, F.; Berki, D.; Damian, D.; Niculite, C.M.; Florea, A.; Leabu, M. *Helleborus purpurascens*—Amino acid and peptide analysis linked to the chemical and antiproliferative properties of the extracted compounds. *Molecules* **2015**, *20*, 22170–22187. [CrossRef]
39. Kostadinova, E.; Nikolova, D.; Alipieva, K.; Stefova, M.; Stefkov, G.; Evstatieva, L.; Matevski, V.; Bankova, V. Chemical constituents of the essential oils of *Sideritis scardica* Griseb. and *Sideritis raeseri* Boiss and Heldr. from Bulgaria and Macedonia. *Nat. Prod. Res.* **2007**, *21*, 319–323. [CrossRef] [PubMed]
40. Kaparakou, E.H.; Daferera, D.; Kanakis, C.D.; Skotti, E.; Kokotou, M.G.; Tarantilis, P.A. Chemical composition of the essential oils of three popular *Sideritis* species cultivated in Greece using GC-MS analysis. *Biomolecules* **2023**, *13*, 1157. [CrossRef]
41. Mróz, M.; Bartoszek, A.; Kusznierevicz, B. Comparative study on assisted solvent extraction techniques for the extraction of biologically active compounds from *Sideritis raeseri* and *Sideritis scardica*. *Molecules* **2023**, *28*, 4207. [CrossRef]
42. Lytra, K.; Tomou, E.; Chrysargyris, A.; Drouza, C.; Skaltsa, H.; Tzortzakakis, N. Traditionally used *Sideritis cypria* Post.: Phytochemistry, nutritional content, bioactive compounds of cultivated populations. *Front. Pharmacol.* **2020**, *11*, 529498. [CrossRef]
43. Tadić, V.; Bojović, D.; Arsić, I.; Đorđević, S.; Aksentijević, K.; Stamenić, M.; Janković, S. Chemical and antimicrobial evaluation of supercritical and conventional *Sideritis scardica* Griseb., Lamiaceae extracts. *Molecules* **2012**, *17*, 2683–2703. [CrossRef]
44. Qazimi, B.; Stefkov, G.; Karapandzova, M.; Cvetkovikj, I.; Kulevanova, S. Aroma compounds of mountain tea (*Sideritis scardica* and *S. raeseri*) from western Balkan. *Nat. Prod. Commun.* **2014**, *9*, 1369–1372. [CrossRef] [PubMed]
45. Todorova, M.; Trendafilova, A. *Sideritis scardica* Griseb., an endemic species of Balkan peninsula: Traditional uses, cultivation, chemical composition, biological activity. *J. Ethnopharmacol.* **2014**, *152*, 256–265. [CrossRef] [PubMed]
46. Romanucci, V.; Di Fabio, G.; D’Alonzo, D.; Guaragna, A.; Scapagnini, G.; Zarrelli, A. Traditional uses, chemical composition and biological activities of *Sideritis raeseri* Boiss. & Heldr. *J. Sci. Food Agric.* **2016**, *97*, 373–383. [PubMed]
47. Deveci, E.; Tel-Çayan, G.; Usluer, Ö.; Duru, M.E. Chemical composition, antioxidant, anticholinesterase and anti-tyrosinase activities of essential oils of two *Sideritis* species from Turkey. *Iran. J. Pharm. Res. IJPR* **2019**, *18*, 903–913. [PubMed]
48. EMA/HMPC/39455/2015. Committee on Herbal Medicinal Products (HMPC) Assessment report on *Sideritis scardica* Griseb. *Sideritis clandestina* (Bory & Chaub.) Hayek; *Sideritis raeseri* Boiss. & Heldr.; *Sideritis syriaca* L., herba, 2016:1–30. Available online: https://www.ema.europa.eu/en/documents/herbal-report/final-assessment-report-sideritis-scardica-griseb-sideritis-clandestina-bory-chaub-hayek-sideritis-raeseri-boiss-heldr-sideritis-syriaca-l-herba_en.pdf (accessed on 24 June 2023).
49. Bojovic, D.; Jankovic, S.; Potpara, Z.; Tadic, V. Summary of the phytochemical research performed to date on *Sideritis* species. *Serbian J. Exp. Clin. Res.* **2011**, *12*, 109–122. [CrossRef]
50. Begas, E.; Kilindris, T.; Kouvaras, E.; Tsioutsoumi, A.; Kouretas, D.; Asproдини, E.K. Dietary effects of *Sideritis scardica* “mountain tea” on human in vivo activities of xenobiotic metabolizing enzymes in healthy subjects. *Food Chem. Toxicol.* **2018**, *122*, 38–48. [CrossRef] [PubMed]
51. Segneanu, A.E.; Marin, C.N.; Ghirlea, O.F.; Feier, C.V.I.; Muntean, C.; Grozescu, I. *Artemisia annua* growing wild in Romania—A metabolite profile approach to target a drug delivery system based on magnetite nanoparticles. *Plants* **2021**, *10*, 2245. [CrossRef]
52. Dash, D.K.; Tyagi, C.K.; Sahu, A.K.; Tripathi, V. Revisiting the Medicinal Value of Terpenes and Terpenoids. In *Revisiting Plant Biostimulants*; Meena, V., Ed.; IntechOpen: London, UK, 2022.
53. Liga, S.; Paul, C.; Péter, F. Flavonoids: Overview of biosynthesis, biological activity, and current extraction techniques. *Plants* **2023**, *12*, 2732. [CrossRef]
54. Ullah, A.; Munir, S.; Badshah, S.L.; Khan, N.; Ghani, L.; Poulson, B.G.; Emwas, H.; Jaremko, M. Important flavonoids and their role as a therapeutic agent. *Molecules* **2020**, *25*, 5243. [CrossRef]
55. Gu, C.; Mao, X.; Chen, D.; Yu, B.; Yang, Q. Isoleucine plays an important role for maintaining immune function. *Curr. Protein Pept. Sci.* **2019**, *20*, 644–651. [CrossRef]

56. Dhama, K.; Karthik, K.; Khandia, R.; Munjal, A.; Tiwari, R.; Rana, R.; Khurana, S.K.; Ullah, S.; Khan, R.U.; Alagawany, M.; et al. Medicinal and therapeutic potential of herbs and plant metabolites/Extracts countering viral pathogens-current knowledge and future prospects. *Curr. Drug Metab.* **2018**, *19*, 236–263. [[CrossRef](#)]
57. Lieu, E.L.; Nguyen, T.; Rhyne, S.; Kim, J. Amino acids in cancer. *Exp. Mol. Med.* **2020**, *52*, 15–30. [[CrossRef](#)] [[PubMed](#)]
58. Wei, Z.; Liu, X.; Cheng, C.; Yu, W.; Yi, P. Metabolism of amino acids in cancer. *Front. Cell Dev. Biol.* **2021**, *8*, 603837. [[CrossRef](#)]
59. Pant, A.; Yang, Z. Asparagine: An Achilles heel of virus replication? *ACS Infect. Dis.* **2020**, *6*, 2301–2303. [[CrossRef](#)] [[PubMed](#)]
60. Liang, H.; Ji, K.; Ge, X.; Zhu, J.; Ren, M.; Mi, H. Methionine played a positive role in improving the intestinal digestion capacity, anti-inflammatory reaction and oxidation resistance of grass carp, *Ctenopharyngodon idella*, fry. *Fish Shellfish. Immunol.* **2022**, *128*, 389–397. [[CrossRef](#)] [[PubMed](#)]
61. Melano, I.; Kuo, L.; Lo, C.; Sung, W.; Tien, N.; Su, C. Effects of basic amino acids and their derivatives on SARS-CoV-2 and influenza-a virus infection. *Viruses* **2021**, *13*, 1301. [[CrossRef](#)] [[PubMed](#)]
62. Aiyelabola, T.; Isabirye, D.; Akinkunmi, E.O.; Ogunkunle, O.; Ojo, I. Synthesis, characterization, and antimicrobial activities of coordination compounds of aspartic acid. *J. Chem.* **2016**, *2016*, 7317015. [[CrossRef](#)]
63. Ji, Y.; Hou, Y.; Blachier, F.; Wu, Z. Editorial: Amino acids in intestinal growth and health. *Front. Nutr.* **2023**, *10*, 1172548. [[CrossRef](#)]
64. Cheng, J.; Tang, J.C.; Pan, M.X.; Chen, S.F.; Zhao, D.; Zhang, Y.; Liao, H.B.; Zhuang, Y.; Lei, R.X.; Wang, S.; et al. L-lysine confers neuroprotection by suppressing inflammatory response via microRNA-575/PTEN signaling after mouse intracerebral hemorrhage injury. *Exp. Neurol.* **2020**, *327*, 113214. [[CrossRef](#)]
65. Theodosios-Nobelos, P.; Papagiouvannis, G.; Tziona, P.; Kourounakis, P.N.; Rekka, E.A. Antioxidant serine-(NSAID) hybrids with anti-inflammatory and hypolipidemic potency. *Molecules* **2021**, *26*, 4060. [[CrossRef](#)]
66. Huang, J.; Zhao, D.; Cui, C.; Hao, J.; Zhang, Z.; Guo, L. Research progress and trends of phenylethanoid glycoside delivery systems. *Foods* **2022**, *11*, 769. [[CrossRef](#)]
67. Zhang, Y.; Cai, P.; Cheng, G.; Zhang, Y. A brief review of phenolic compounds identified from plants: Their extraction, analysis, and biological activity. *Nat. Prod. Commun.* **2022**, *17*, 1934578X211069721. [[CrossRef](#)]
68. Wang, C.; Gong, X.; Bo, A.; Zhang, L.; Zhang, M.; Zang, E.; Zhang, C.; Li, M. Iridoids: Research advances in their phytochemistry, biological activities, and pharmacokinetics. *Molecules* **2020**, *25*, 287. [[CrossRef](#)] [[PubMed](#)]
69. Baumel, B.S.; Doraiswamy, P.M.; Sabbagh, M.; Wurtman, R. Potential neuroregenerative and neuroprotective effects of uridine/choline-enriched multinutrient dietary intervention for mild cognitive impairment: A narrative review. *Neurol. Ther.* **2021**, *10*, 43–60. [[CrossRef](#)]
70. Chojnowski, K.; Opielka, M.; Nazar, W.; Kowianski, P.; Smolenski, R.T. Neuroprotective effects of guanosine in ischemic stroke—Small steps towards effective therapy. *Int. J. Mol. Sci.* **2021**, *22*, 6898. [[CrossRef](#)]
71. Das, K.; Gezici, S. Secondary plant metabolites, their separation and identification, and role in human disease prevention. *Ann. Phytomed. Int. J.* **2018**, *7*, 13–24. [[CrossRef](#)]
72. He, M.; Ding, N. Plant unsaturated fatty acids: Multiple roles in stress response. *Front. Plant Sci.* **2020**, *11*, 562785. [[CrossRef](#)]
73. Vezza, T.; Canet, F.; De Marañón, A.M.; Bañuls, C.; Rocha, M.; Víctor, V.M. Phytosterols: Nutritional health players in the management of obesity and its related disorders. *Antioxidants* **2020**, *9*, 1266. [[CrossRef](#)] [[PubMed](#)]
74. Hu, Y.; Lin, Q.; Zhao, H.; Li, X.; Sang, S.; McClements, D.J.; Long, J.; Jin, Z.; Wang, J.; Qiu, C. Bioaccessibility and bioavailability of phytochemicals: Influencing factors, improvements, and evaluations. *Food Hydrocoll.* **2023**, *135*, 108165. [[CrossRef](#)]
75. Catalano, A.; Iacopetta, D.; Ceramella, J.; Scumaci, D.; Giuzio, F.; Saturnino, C.; Aquaro, S.; Rosano, C.; Sinicropi, M.S. Multidrug Resistance (MDR): A Widespread Phenomenon in Pharmacological Therapies. *Molecules* **2022**, *27*, 616. [[CrossRef](#)]
76. Lamptey, R.N.L.; Chaulagain, B.; Trivedi, R.; Gothwal, A.; Layek, B.; Singh, J. A review of the common neurodegenerative disorders: Current therapeutic approaches and the potential role of nanotherapeutics. *Int. J. Mol. Sci.* **2022**, *23*, 1851. [[CrossRef](#)]
77. Stuart, B.H. Infrared Spectroscopy: Fundamentals and applications. In *Analytical Techniques in the Sciences*; John Wiley & Sons, Ltd.: Hoboken, NJ, USA, 2004; ISBN 9780470854273.
78. Yadav, N.; Yadav, R.; Goyal, A. Chemistry of terpenoids. *Int. J. Pharm. Sci. Rev. Res.* **2014**, *27*, 272–278.
79. Segneanu, A.-E.; Marin, C.N.; Herea, D.D.; Stanusoiu, I.; Muntean, C.; Grozescu, I. Romanian *Viscum album* L.—Untargeted low-molecular metabolomic approach to engineered *Viscum*-AuNPs carrier assembly. *Plants* **2022**, *11*, 1820. [[CrossRef](#)] [[PubMed](#)]
80. Xue, Z.; Yang, B. Phenylethanoid glycosides: Research advances in their phytochemistry, pharmacological activity and pharmacokinetics. *Molecules* **2016**, *21*, 991. [[CrossRef](#)]
81. Akcos, Y.; Ezer, N.; Çalis, I.; Demirdamar, R.; Tel, B.C. Polyphenolic compounds of *Sideritis lycia* and their anti-inflammatory activity. *Pharm. Biol.* **1999**, *37*, 118–122. [[CrossRef](#)]
82. Olivier, D.K.; Shikanga, E.A.; Combrinck, S.; Krause, R.W.M.; Regnier, T.; Dlamini, T.P. Phenylethanoid glycosides from *Lippia javanica*. *South Afr. J. Bot.* **2010**, *76*, 58–63. [[CrossRef](#)]
83. Scarsini, M.; Thurotte, A.; Veidl, B.; Amiard, F.; Niepceron, F.; Badawi, M.; Lagarde, F.; Schoefs, B.; Marchand, J. Metabolite quantification by Fourier Transform Infrared Spectroscopy in diatoms: Proof of Concept on *Phaeodactylum tricorutum*. *Front. Plant Sci.* **2021**, *12*, 756421. [[CrossRef](#)]
84. Topală, C.M.; Tătarua, L.D.; Ducu, C. ATR-FTIR spectra fingerprinting of medicinal herbs extracts prepared using microwave extraction. *Arab. J. Med. Aromat. Plants AJMAP* **2017**, *3*, 1–9.
85. Filopoulou, A.; Vlachou, S.; Boyatzis, S.C. Fatty acids and their metal salts: A review of their infrared spectra in light of their presence in cultural heritage. *Molecules* **2021**, *26*, 6005. [[CrossRef](#)] [[PubMed](#)]

86. Krysa, M.; Szymańska-Chargot, M.; Zdunek, A. FT-IR and FT-Raman fingerprints of flavonoids—A review. *Food Chem.* **2022**, *393*, 133430. [[CrossRef](#)] [[PubMed](#)]
87. Bensemmane, N.; Bouzidi, N.; Daghbouche, Y.; Garrigues, S.; Guardia, M.; El Hattab, M. Quantification of phenolic acids by partial least squares Fourier-transform infrared (PLS-FTIR) in extracts of medicinal plants. *Phytochem. Anal.* **2021**, *32*, 206–221. [[CrossRef](#)]
88. Akbari, S.; Abdurahman, N.H.; Fayaz, F.; Noory, V. Iridoids of fenugreek (*Trigonella-foenum-graecum* L.) seed extract detected via LC-QTOF-MS analysis. *Future Foods* **2021**, *4*, 100067. [[CrossRef](#)]
89. Pang, M.; Jiang, S.; Cao, L.; Pan, L. Novel synthesis of steryl esters from phytosterols and amino acid. *J. Agric. Food Chem.* **2011**, *59*, 10732–10736. [[CrossRef](#)]
90. Mukesh, K.K.; Manoj, S.; Agrawal, R.D. Isolation and identification of phytosterols from leaves of *Maytenus emarginata* plant. *Int. J. Educ. Mod. Manag. Appl. Sci. Soc. Sci. (IJEMASSS)* **2021**, *3*, 291–296.
91. Segneanu, A.; Velcirov, S.M.; Olariu, S.; Cziple, F.; Damian, D.; Grozescu, I. Bioactive molecules profile from natural compounds. In *Amino Acid—New Insights and Roles in Plant and Animal*; Asao, T., Asaduzzaman, M., Eds.; IntechOpen: Rijeka, Croatia, 2017.
92. Olejniczak, A.B.; Sut, A.; Wróblewski, A.E.; Leśnikowski, Z.J. Infrared spectroscopy of nucleoside and DNA-oligonucleotide conjugates labeled with carborane or metallacarborane cage. *Vib. Spectrosc.* **2005**, *39*, 177–185. [[CrossRef](#)]
93. Mozgawa, W.; Król, M.; Barczyk, K. FT-IR studies of zeolites from different structural groups. *Chemik* **2011**, *65*, 667–674.
94. Korkuna, O.; Lebeda, R.; Skubiszewska-Zieba, J.; Vrublevska, T.; Gunko, V.M.; Ryczkowski, J. Structural and physicochemical properties of natural zeolites: Clinoptilolite and mordenite. *Microporous Mesoporous Mater.* **2006**, *87*, 243–254. [[CrossRef](#)]
95. Segneanu, A.E.; Trusca, R.; Cepan, C.; Mihailescu, M.; Muntean, C.; Herea, D.D.; Grozescu, I.; Salifoglou, A. Innovative low-cost composite nanoadsorbents based on eggshell waste for nickel removal from aqueous media. *Nanomaterials* **2023**, *1*, 2572. [[CrossRef](#)] [[PubMed](#)]
96. Ali, A.; Chiang, Y.W.; Santos, R.M. X-ray diffraction techniques for mineral characterization: A review for engineers of the fundamentals, applications, and research directions. *Minerals* **2022**, *12*, 205. [[CrossRef](#)]
97. Senila, M.; Neag, E.; Cadar, O.; Hoaghia, M.A.; Roman, M.; Moldovan, A.; Hosu, A.; Lupas, A.; Kovacs, E.D. Characteristics of volcanic tuff from Macicasu (Romania) and its capacity to remove ammonia from contaminated Air. *Molecules* **2022**, *27*, 3503. [[CrossRef](#)] [[PubMed](#)]
98. Güngör, D.; Özen, S. Development and characterization of clinoptilolite-, mordenite-, and analcime-based geopolymers: A comparative study. *Case Stud. Constr. Mater.* **2021**, *15*, e00576. [[CrossRef](#)]
99. Segneanu, A.E.; Vlase, G.; Lukinich-Gruia, A.T.; Herea, D.D.; Grozescu, I. Untargeted metabolomic approach of *Curcuma longa* to neurodegenerative phytocarrrier system based on silver nanoparticles. *Antioxidants* **2022**, *11*, 2261. [[CrossRef](#)]
100. Goetze, J.; Yarulina, I.; Gascon, J.; Kapteijn, F.; Weckhuysen, B.M. Revealing lattice expansion of small-pore zeolite catalysts during the methanol-to-olefins process using combined operando X-ray diffraction and UV-vis spectroscopy. *ACS Catal.* **2018**, *8*, 2060–2070. [[CrossRef](#)]
101. Kadja, G.T.; Culsum, N.T.; Putri, R.M. Recent advances in the utilization of zeolite-based materials for controlled drug delivery. *Results Chem.* **2022**, *5*, 100910. [[CrossRef](#)]
102. Abukhadra, R.A.; Adlii, A.; Khim, J.; Ajarem, J.; Allam, A. Insight into the technical qualification of the sonocogreen CaO/Clinoptilolite nanocomposite (CaO (NP) /Clino) as an advanced delivery system for 5-fluorouracil: Equilibrium and cytotoxicity. *ACS Omega* **2021**, *6*, 31982–31992. [[CrossRef](#)]
103. Díaz, M.J.; Ruiz-Montoya, M.; Palma, A.; de-Paz, M.V. Thermogravimetry applicability in compost and composting research: A review. *Appl. Sci.* **2021**, *11*, 1692. [[CrossRef](#)]
104. Fernandes, F.H.A.; Santana, C.P.; Santos, R.L.; Correia, L.P.; Conceição, M.M.; Macêdo, R.O.; Medeiros, A.C.D. Thermal characterization of dried extract of medicinal plant by DSC and analytical techniques. *J. Therm. Anal. Calorim.* **2012**, *113*, 443–447. [[CrossRef](#)]
105. Dinkova-Kostova, A.T.; Talalay, P. Direct and indirect antioxidant properties of inducers of cytoprotective proteins. *Mol. Nutr. Food Res.* **2008**, *52*, S128–S138. [[CrossRef](#)] [[PubMed](#)]
106. Amorati, R.; Valgimigli, L. Methods to measure the antioxidant activity of phytochemicals and plant extracts. *J. Agric. Food Chem.* **2018**, *66*, 3324–3329. [[CrossRef](#)]
107. Losada-Barreiro, S.; Sezgin-Bayindir, Z.; Paiva-Martins, F.; Bravo-Díaz, C. Biochemistry of antioxidants: Mechanisms and pharmaceutical applications. *Biomedicines* **2022**, *10*, 3051. [[CrossRef](#)] [[PubMed](#)]
108. Gulcin, İ. Antioxidants and antioxidant methods: An updated overview. *Arch.Toxicol.* **2020**, *94*, 651–715. [[CrossRef](#)] [[PubMed](#)]
109. Flieger, J.; Flieger, W.; Baj, J.; Maciejewski, R. Antioxidants: Classification, natural sources, activity/capacity measurements, and usefulness for the synthesis of nanoparticles. *Materials* **2021**, *14*, 4135. [[CrossRef](#)] [[PubMed](#)]
110. Mbinda, W.; Musangi, C. Antioxidant activity, total phenolic and total flavonoid contents of stem bark and root methanolic extracts of *Calotropis procera*. *J. Phytopharm.* **2019**, *8*, 161–166. [[CrossRef](#)]
111. Segneanu, A.E.; Vlase, G.; Vlase, T.; Sicoe, C.A.; Ciocalteu, M.V.; Herea, D.D.; Ghirlea, O.F.; Grozescu, I.; Nanescu, V. Wild-grown Romanian *Helleborus purpurascens* approach to novel chitosan phyto-nanocarriers—Metabolite profile and antioxidant properties. *Plants* **2023**, *12*, 3479. [[CrossRef](#)]

112. El-Sawi, S.A.; Motawae, H.M.; Abdelkawy, M.A.; Fekry, M.I.; Youssef, H.F.; Farghaly, A.A.; Maamoun, M.A. Novel anticancer drug delivery system based on zeolite encapsulating *Hamelia patens* leaf and flower extracts. *Indian J. Nat. Prod. Resour.* **2021**, *12*, 181–194.
113. Mbamalu, O.N.; Syce, J.; Samsodien, H. Short communication. challenges relating to comparison of flavonoid glycosides dissolution profiles from *Sutherlandia frutescens* products. *Acta Pharm.* **2017**, *67*, 137–146. [[CrossRef](#)]
114. Pranskuniene, Z.; Bernatoniene, J.; Kalveniene, Z.; Masteikova, R.; Mekas, T.; Velziene, S.; Ivanauskas, K.; Suchockas, V.; Mintauckiene, I.; Savickas, A. New formula herbal pellets demonstrate a uniform and stable release of the active ingredients in vitro. *Acta Pol Pharm.* **2013**, *70*, 727–736.
115. Sharma, R.; Ashawat, M.S.; Verma, C.P.S.; Kumari, N. A fast release tablet containing Herbal extracts (ginger, cinnamon, turmeric, long pepper and punarnava). *Asian J. Pharm. Tech.* **2020**, *10*, 231–240. [[CrossRef](#)]
116. Osei-Asare, C.; Akuffo Owusu, F.W.; Entsie, P.; Kwansima Annan, A.; Akosua Gyamaa, R.; Makafui Amenuke, E. Formulation and in vitro evaluation of oral capsules from liquid herbal antimalarials marketed in Ghana. *Hindawi J. Trop. Med.* **2021**, *2021*, 6694664. [[CrossRef](#)]
117. Hussain, A.; Attique, F.; Naqvi, S.A.R.; Ali, A.; Ibrahim, M.; Hussain, H.; Zafar, F.; Iqbal, R.S.; Ayub, M.A.; Assiri, M.A.; et al. Nanoformulation of *Curcuma longa* root extract and evaluation of its dissolution potential. *ACS Omega* **2022**, *8*, 1088–1096. [[CrossRef](#)]
118. Chowdary, H.V.; Venkaiah, A.; Malik, S.V.; Reddy, H.S.; Achari, S.V.; Raju, P.Y. Dissolution test as a quality control tool for herbal formulations—A comprehensive review. *Int. J. Innov. Pharm. Res.* **2014**, *5*, 364–369.
119. Lex, T.R.; Rodriguez, J.D.; Zhang, L.; Jiang, W.; Gao, Z. Development of in vitro dissolution testing methods to simulate fed conditions for immediate release solid oral dosage forms. *AAPS J.* **2022**, *24*, 40. [[CrossRef](#)] [[PubMed](#)]
120. Wang, M.; Jin, X.; Ren, X.; Zhu, Y.; Liu, Z.; Gao, X. Comparative in vitro dissolution of two commercially available Er-Zhi-Wan herbal medicinal products. *Indian J. Pharm. Sci.* **2015**, *77*, 391–398.
121. Aswathy, K.; Asdaq, S.M.B.; Saritha, C.; Thomas, L.; Haridas, N.; Viswanad, V.; Sahu, R.K.; Fattepur, S.; Alamri, A.S.; Alsanie, W.F.; et al. Formulation and in-vitro characterization of fast-disintegrating herbal extract sublingual immunotherapy tablet for peanut-induced allergic asthma. *Saudi J. Biol. Sci.* **2022**, *29*, 1283–1297. [[CrossRef](#)] [[PubMed](#)]
122. Medina-Remón, A.; Barrionuevo-González, A.; Zamora-Ros, R.; Andres-Lacueva, C.; Estruch, R.; Martínez-González, M.Á.; Diez-Espino, J.; Lamuela-Raventos, R.M. Rapid Folin–Ciocalteu method using microtiter 96-well plate cartridges for solid phase extraction to assess urinary total phenolic compounds, as a biomarker of total polyphenols intake. *Anal. Chim. Acta* **2009**, *634*, 54–60. [[CrossRef](#)] [[PubMed](#)]
123. Surat, P. pH in the Human Body. News-Medical, 10 October 2022. Available online: <https://www.news-medical.net/health/pH-in-the-Human-Body.aspx> (accessed on 16 November 2023).
124. Anumolu, P.D.; Gurralla, S.; Venkata Satya, S.C.; Polisetty, S.V.; Ravindran, A.; Achanta, R. Development of a discriminative and biorelevant dissolution test method for atorvastatin/fenofibrate combination with appliance of derivative *spectrophotometry*. *Turk. J. Pharm. Sci.* **2019**, *16*, 62–68. [[CrossRef](#)]
125. Mureşan, M.; Olteanu, D.; Filip, G.A.; Clichici, S.; Baldea, I.; Jurca, T.; Pallag, A.; Marian, E.; Frum, A.; Gligor, F.G.; et al. Comparative study of the pharmacological properties and biological effects of *Polygonum aviculare* L. herba extract-entrapped liposomes versus quercetin-wntrapped liposomes on doxorubicin-induced toxicity on HUVECs. *Pharmaceutics* **2021**, *13*, 1418. [[CrossRef](#)]

Disclaimer/Publisher’s Note: The statements, opinions and data contained in all publications are solely those of the individual author(s) and contributor(s) and not of MDPI and/or the editor(s). MDPI and/or the editor(s) disclaim responsibility for any injury to people or property resulting from any ideas, methods, instructions or products referred to in the content.